

THE UNIVERSITY OF CALGARY

Validation Of Chemical Shift Imaging Against Organic Solvent Lipid

Extraction: Quantification Of Lipid In Cadaveric Skeletal Muscle

by

Steven B. Hudson

A THESIS

SUBMITTED TO THE FACULTY OF GRADUATE STUDIES

IN PARTIAL FULFILLMENT OF THE REQUIREMENTS FOR THE

DEGREE OF MASTER OF SCIENCE

DEPARTMENT OF KINESIOLOGY

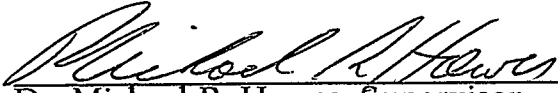
CALGARY, ALBERTA

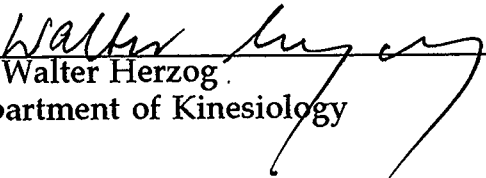
JUNE, 1996

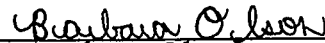
© Steven B. Hudson 1996

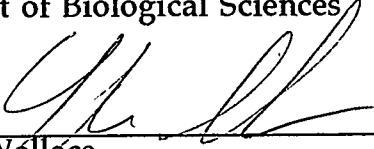
THE UNIVERSITY OF CALGARY
FACULTY OF GRADUATE STUDIES


The undersigned certify that they have read, and recommend to the Faculty of Graduate Studies for acceptance, a thesis entitled "Validation Of Chemical Shift Imaging Against Organic Solvent Lipid Extraction: Quantification Of Lipid In Cadaveric Skeletal Muscle" submitted by Steven Hudson in partial fulfillment of the requirements for the degree of Master of Science.


Dr. Michael R. Hawes, Supervisor
Department of Kinesiology


Dr. Walter Herzog
Department of Kinesiology


Dr. Barbara Olson
Department of Biological Sciences


Dr. Carla Wallace
Department of Radiology, Foothills Hospital


Dr. Alan Martin
External Examiner
School of Human Kinetics
University of British Columbia

June 27, 1996

Abstract

The purpose of this thesis was to validate a method for quantifying the lipid component of cadaveric human skeletal muscle. An experimental and control method were compared. The experimental method was a modification of conventional magnetic resonance imaging known as chemical shift imaging (CSI), which images protons at the water/fat chemical shift. Subsequent analysis of the CSI data determined lipid content. The control method was organic solvent lipid extraction (LE). Six unembalmed cadavers, five female and one male (age range of 80 to 97 years), were imaged using the experimental protocol. Muscle tissue was subsequently dissected, homogenized and subjected to LE procedures.

The results suggested agreement between the methods. A plot of the data and subsequent analysis resulted in a slope of zero with limits of agreement (mean \pm 2 sd) of 9.27 to -10.04. A 95 percent confidence interval was calculated to account for sample size and was 1.59 to -2.35. A paired t-test was not significant ($t_{(23)} = 0.39$) $p = 0.35$. Mean values of the percent lipid extracted using the experimental method resulted in a range of 4.36 to 12.95. Values for the same samples obtained by the control method ranged from 5.06 to 15.01 percent. A comparison of mean percent lipid content of dissected cadaver muscle tissue and whole body adiposity moderately correlated ($r=0.58$). The comparison of lipid content to directly measured regional adiposity resulted in a poor ($r = 0.14$) correlation.

Acknowledgments

I would like to thank the following individuals and groups for their assistance in the completion of this thesis:

Dr. Michael Hawes for his confidence, direction and patience. Also, for his efforts in providing me with the many opportunities which have given me invaluable experience and truly contributed to my overall education.

The members of my examining committee: Dr. Walter Herzog, Dr. Barb Olson, Dr. Carla Wallace and Dr. Alan Martin.

Pierre LaForge for his technical expertise and dedication to his profession.

Dr. Adrian Crawley for introducing me to magnetic resonance imaging and his effort and time in "making it all work".

Yan Hui for answering my many questions and his expertise in image analysis.

The Olympic Oval Fund for their financial support.

To the individuals who have unselfishly given their bodies to further mankind's understanding of himself.

My wife, Karen for her love and support and our children, Zachary and Rachel, for their understanding of my absence from home while at the "Versity" preparing the manuscript.

Table of Contents

Approval Page	ii
Abstract	iii
Acknowledgments	iv
Table of Contents	v
List of Tables	viii
List of Figures	ix
INTRODUCTION	1
1.1 Estimation of Muscle Mass	2
1.2 Nuclear Magnetic Resonance, Magnetic Resonance Imaging and Chemical Shift Imaging	4
1.3 Statement Of The Problem	5
1.4 Purpose of the Study	6
1.5 Statement Of Research Hypothesis	7
LITERATURE REVIEW	8
2.1 Basic Principles of Magnetic Resonance Imaging	8
2.2 Clinical Use of Magnetic Resonance imaging	10
2.3 Chemical Shift Imaging	11
2.3.1 Selective Saturation and Excitation, and CSI	13
2.3.2 Modified Conventional MRI and CSI	15
2.3.3 Other CSI Techniques	17
2.4 Lipid quantification in Biological tissues using CSI	17
2.5 Quantification of Adipose Tissue using MRI	18

2.6 Lipid Definition and Background	19
2.7 Lipid Quantification in Body Composition	20
2.7.1 Lean-Body Mass vs. Fat-Free Mass	21
METHODOLOGY	25
3.1 Cadaveric Specimens	25
3.1.1 Specimen Acceptance	26
3.2 Specimens	26
3.3 General Overview of Method	28
3.4 Specific Procedures	30
3.4.1 Anthropometric Procedures	30
3.4.2 Regional Site Landmarks	32
3.5 Equipment	32
3.6 Sample Preparation	32
3.7 Magnetic Resonance Data Collection	34
3.8 Magnetic Resonance Data Analysis	36
3.9 Lipid Extraction	37
3.10 Statistical Analysis	39
RESULTS	41
4.1 Anthropometry	41
4.1.1 Adiposity	41
4.1.2 Direct AT Measures	43
4.1.3 Muscle Mass	43
4.1.4 Skeletal Mass Estimation	45

4.2 Comparison of Methods	46
4.2.1 Descriptive Analysis	46
4.2.2 Assessment of Agreement	48
4.2.3 Paired student's t-test	50
4.2.4 Correlation	50
DISCUSSION	51
5.1 Magnetic Resonance Imaging Methods	51
5.1.1 Conventional MRI	52
5.1.2 Chemical Shift Imaging	54
5.2 Agreement of Methods	54
5.2.1 Descriptive Data	54
5.2.2 Statistical Procedures	57
5.3 CSI Limitations	59
5.4 Body Composition	60
5.5 Relationships Between Intra- and Extra-cellular Lipid and Other Fat Depots	61
5.6 Future Considerations	62
5.7 Conclusion	63
REFERENCES	64
APPENDIX A	74
APPENDIX B	82
APPENDIX C	90
APPENDIX D	103

List of Tables

1	Tissue mass distribution	23
2	Specimen demographics	27
3	Sites for measurements of girths, breadths and skinfolds	31
4	Specimen adiposity values	42
5	Sum of four (anterior, posterior, lateral and medial) direct AT measurements	44
6	Estimation of specimen muscle mass	45
7	Estimation of specimen skeletal mass	46
8	Comparison of percent lipid using magnetic resonance (CSI) and organic solvent LE methods	47

List of Figures

1	Schematic drawing of specimen set-up on MRI table	35
2	Flowchart of magnetic resonance data	38
3	Flowchart of the lipid extraction	40
4	Difference of percent lipid (CSI - LE) against mean percent lipid (CSI + LE)/2	49
5	Photographs of upper leg segment comparing AT within muscle between two specimens	56

CHAPTER ONE

INTRODUCTION

Research in the field of body composition has focused primarily on the quantity and deposition of fat in the human body. This may be founded in the fact that adipose was the first tissue studied in the modern era of body composition (Behnke, 1942). More recently, this trend has been propagated by research which indicates that excess adipose tissue may have a negative relationship to health, quality of life and sport performance.

It is evident to the health and sport performance professions that the determination of changing regional and total quantities of muscle mass are also significant variables in quantitative anatomical research. For example, quantifying skeletal muscle has been shown to be well suited for determining the severity of lean tissue depletion as a result of protein energy malnutrition and could be effectively used to observe the recovery process of associated conditions (Heymsfield et al., 1982a). In the area of sport performance, Spenst, Martin & Drinkwater (1993), suggest that since athletes in various sports show greater variability in muscle mass than in fat mass, measurement of the former could be useful in the selection, training and monitoring of athletes.

Fundamental to the general approach of the present research, is the concept that this research will allow further and more precise quantification

of the constituents in human skeletal muscle. Further, the present study will forward research in the field of kinanthropometry and contribute towards greater understanding of human body composition.

1.1 Estimation of Muscle Mass

There are several laboratory and field tests which estimate muscle mass. These tests employ both anatomical (tissue based) and molecular (cell based) models. Anatomically based models have been proposed by Matiegka (1921), Heymsfield et al. (1982b), Drinkwater et al. (1986), and Martin (1990). These models are based on the assumption that extremity girths can be represented as a circle and that a single skinfold thickness is representative of a constant subcutaneous layer overlying a circular muscle mass. Thus, by measuring the girth and skinfold thickness of the extremity and using circle geometry, an estimate of total muscle cross-sectional area can be achieved. These methods lack formal quantification of any lipids at the molecular level which may be found within the muscle tissue such as those present in the fascia or the cell walls, and any adipose tissue surrounding vessels and nerves embedded within the muscle groups.

Two laboratory methods exist which are based on the molecular model. The most common of these involves the measurement of urine creatinine in a 24-hour sample. Creatinine is a nitrogenous organic acid synthesized from four amino acids and is largely located in muscle (98 percent of the creatinine

pool) (Heymsfield, 1983). Its only metabolic waste is creatinin which passes unaltered through the kidney. A creatinin assay of a 24-hour urine sample will reflect total body creatin, from which an estimation of total body muscle mass may be obtained. The second method measures an amino acid, 3-methyl histidine, which is found almost exclusively in myofibrillar protein. During catabolism, 3-methyl histidine is neither recycled for protein synthesis nor metabolized further and is excreted via the urine. Work by Mendez et al. (1984) showed that muscle protein metabolism should be a balanced process during steady state and therefore 3-methyl histidine could be assayed to estimate total body muscle mass.

These methods are limited by several factors. 24-hour urine creatinine measurement can vary due to factors which may lack experimental control such as; diet, strenuous exercise, emotional stress and menstruation. Both of these methods are based on animal models and do not have established definitive equivalence values. Further, there are relatively severe restrictions placed on subjects, including the absolute collection of urine for 24-hours and diet restrictions. Finally, the validation of these methods has been against other biochemical methods which lack direct validation.

With the exception of a single method (Martin et al., 1990), muscle mass has been estimated using methods which lack direct validation. The methods outlined above center around the relationship between measurable parameters such as girths, skinfold thicknesses, and metabolic wastes with

muscle mass and they are based on empirical regression equations. In addition, there are other assumptions which have not been validated by any of the foregoing methods. One of these assumptions is that the amount of lipid contained in skeletal muscle is either negligible or constant and therefore need not be considered when estimating muscle mass. In the past, a lack of appropriate technology has been a great inhibitor in the validation of this assumption. However, recent advances in nuclear magnetic resonance imaging (MRI) and computer technology allow the opportunity to quantify the amount of lipid found in and around skeletal muscle.

1.2 Nuclear Magnetic Resonance, Magnetic Resonance Imaging and Chemical Shift Imaging

Nuclear magnetic resonance (NMR) has been widely used as a spectroscopic technique (Pykett et al., 1982; Dixon, 1984), to obtain information on the structure of chemicals and the nature of static and dynamic interactions between molecular nuclei in a wide variety of materials and biological systems (Pykett et al., 1982). In the early 1980's NMR principles were used to develop an imaging technique known as MRI. Since that time MRI has gained credibility and wide spread use as an imaging technique. A combination of NMR principles and MRI technology now allows information previously shown as spectra to be seen as images at specified chemical shifts, using a technique known as Chemical Shift Imaging (CSI).

As most of the nuclear magnetization of the body comes from hydrogen nuclei in water, and most of the remainder from hydrogen protons in fat, a simple approach may allow quantification of the amount of fat in a given tissue by simple mathematics. CSI provides a precise method to quantify methylene protons (hydrogen protons associated with fat) and therefore increases the contrast between fat-containing tissues and others, allowing detection of smaller masses of fat in a given tissue. This technique is non-invasive and has no known side-effects, therefore it becomes a method which may be used both *in vitro* and *in vivo*.

1.3 Statement Of The Problem

The quantity of lipid found within fascial boundaries of muscle, including muscle fibers, fasciculi and stroma has not been determined. In the past, the lack of knowledge regarding quantification of cellular and extracellular lipid within muscle tissue has been regarded as unavailing to research in body composition.

Previous lipid classification and quantification from various tissues, including skeletal muscle of various mammals and human cadavers, has included the use of organic solvents such as methanol, chloroform and ether (Forbes, Cooper & Mitchell, 1953; Forbes, Mitchell & Cooper, 1956; Mitchell, 1945; Moore et al., 1968; Widdowson, McCance & Spray, 1951). These methods of determining cellular and extracellular lipid have not been used for *in vivo*

human research because a sizable sample of excised tissue is required. However, using a cadaveric specimen, the organic solvents methods provide an excellent standard by which to compare new methods as they are simple to perform and inexpensive to prepare. Further, the use of organic solvents to extract lipids from various tissues is founded on basic biochemical principles and has been shown to yield less than five percent loss of total lipid (Folch, Lees and Slone, 1956; Mangold, 1984).

1.4 Purpose of the Study

The purpose of this study was two-fold. The primary focus was to validate the use of an MRI protocol as a viable method of determining the quantity of lipids found within the facial boundaries of human skeletal muscle. This involves spatial mapping of data on the chemical shift between water and fat at several representative sites in a sample population of human cadavers.

The secondary focus was to investigate the possible relationship between anthropometric measures of adiposity and MRI measures of cellular and extracellular lipids found within cadaveric skeletal muscle.

1.5 Statement Of Research Hypothesis

The mean values of cellular and extracellular lipid within muscle tissue as determined by CSI using a modified Dixon (1984) double phase

contrast acquisition protocol, will not be significantly different from the mean values of cellular and extracellular lipids within muscle tissue obtained by lipid extraction (Mangold, 1984) using organic solvents.

A second hypothesis states that a strong relationship as determined by correlations between the estimates of regional and whole body adiposity and MRI measures of cellular and extracellular lipids in muscle will exist.

CHAPTER TWO

LITERATURE REVIEW

NMR is the physical process upon which MRI is based. It was first recognized in 1946 and was used largely as an analytical tool in chemistry for the next 30 years (Oldendorf and Oldendorf, 1991). The term NMR is still used today in analytical chemistry. The term NMR was initially applied to scanners used in the clinical setting, but by convention MRI is currently used since the word 'nuclear' caused concern among patients.

2.1 Basic Principles of Magnetic Resonance Imaging

NMR of the human body and subsequent magnetic resonance imaging of the body can best be understood with a general description of magnets and their interaction with magnetic fields. A magnet will align itself within a given field. A common example of this is a compass needle aligning in the magnetic field of the earth. If a compass needle at rest receives a tap on one end of the needle, the needle will first deflect away from north but will be drawn back to north. Upon return, the needle overshoots north, and will continue to oscillate back and forth, gradually diminishing in magnitude until all the energy the needle received from the tap is lost. The frequency of this oscillatory movement is referred to as the needle's natural frequency or

resonant frequency. Natural frequency depends on an object's dimensions, strength of magnetization, and mass, and on the strength of the magnetic field. The natural frequency of a magnet is proportional to the strength of a magnetic field, therefore if a magnetic field doubles in strength, the natural frequency of the magnet doubles.

The location of a magnet can therefore be determined if the gradient or change in magnetic field strength is known. In the compass example, the earth's magnetic field is not uniform over its entire surface. For instance, the north pole has a magnetic strength of 0.7 gauss, whereas at the equator it is 0.3 gauss. Therefore given a compass with a natural frequency of 1.0 Hz at the equator, one could navigate to the north pole where the compass would have a natural frequency of 2.3 Hz.

Of the 280 combinations of protons and neutrons (elements), approximately 100 are magnetic (Oldendorf and Oldendorf, 1991). Of these, hydrogen is of the greatest biological interest (Bottomley, Foster & Leue, 1984; Wong et al., 1994; Dixon, 1984). It is abundant, making up approximately two-thirds of the atoms in living tissues and it is highly magnetic. In the body, hydrogen nuclei also known as 'dipoles' or 'spins', act as tiny magnets and can be compared to the needle of a compass. When they are not exposed to a strong external magnetic field these dipoles are aligned randomly. When a body or biological specimen is placed in a strong magnetic field, the dipoles align with or against the external magnetic field, resulting in a small net

magnetization (M_0) in the direction of the external magnetic field. The M_0 vector is a vector sum of the magnetization contributed by the dipoles associated with water and the dipoles associated with fat. In each case the alignment is not perfect, rather the dipoles precess around this vector, with water precessing faster than fat. The dipoles have a resonant frequency that is proportional to the external magnetic field, they absorb energy, and in turn re-emit energy.

2.2 Clinical Use of Magnetic Resonance imaging

Non-invasive medical imaging technology, including MRI, has developed at a very rapid rate in the last decade. Magnetic resonance has been and continues to be used extensively as a spectroscopic technique in non-medical fields and has grown into a widely used imaging technique in medicine. The practical combination of these two approaches, CSI, was shown to be of significant use about ten years ago and has been demonstrated on the nuclei of hydrogen (Pykett & Rosen, 1983; Bottomley, 1984; Dixon, 1984; Sepponen, Sipponen, & Tanttu, 1984; Haase, 1985; Joseph, 1985), deuterium (Cox & Styles, 1980), carbon (Ackerman et al., 1980; Alger et al., 1981), and P-31 (Gordon et al., 1980; Brown, Kincaid, & Ugurbil, 1982). Particularly of interest, is the ability of this combination to detect smaller masses of fat within tissue (Heiken et al., 1984; Lee et al., 1984; Matthaei, 1984; Sepponen et al., 1984; Joseph, 1985).

2.3 Chemical Shift Imaging

The Larmor equation $\omega = \gamma \beta_0$ describes the relationship among the Larmor frequency of the proton of interest, ω , the gyromagnetic ratio of the nucleus, γ , and the strength of the external magnet, β_0 . However, the field in which the nucleus is situated, is different from the field created by the external magnet alone. This difference is due to a net magnetization in the body or tissue which is created as the hydrogen dipoles align themselves within the applied external magnetic field. The resultant effect is one of shielding the nucleus from the applied magnetic field. Thus, a particular nucleus of a given species, placed in a known-strength external magnetic field can have different resonance frequencies, dependent on the surrounding chemical environment. This phenomenon allows the observation of a spectrum of resonance frequencies for a given atom in various molecules.

In conventional MRI no distinction is made with regard to the chemical environments associated with the various hydrogen atoms of the body. However, hydrogen atoms associated with aliphatic carbon chains found in the fatty acid tails of lipids or tissues such as fat, resonate at a different frequency than hydrogen nuclei associated with water molecules. Determining the spatial distribution of these different hydrogen nuclei, rather than imaging the entire spectrum of resonance frequencies within a tissue/body is called CSI.

Chemical shifts are generally expressed in terms of parts per million (ppm) because the actual frequency difference depends on the external magnetic field strength. A magnetic field (0.35 T) in which hydrogen atoms in lipids resonate at 15 000 000 hertz allows protons in water to resonate at 15 000 050 hertz. The chemical shift difference between protons associated with lipid and those associated with water is 50 hertz per 15 megahertz, or 3.3 ppm (Dixon, 1984).

The total frequency range of the chemical shift for a given nucleus depends on both field strength and the isotope being studied. The total range of chemical shifts, expressed in ppm, is therefore different for various isotopes (Pykett et al., 1982). For hydrogen the range is 12 ppm, while ^{19}F has a range of approximately 300 ppm and ^{31}P about 320 ppm. In spectroscopy, greater range is more desirable as the signal to noise ratio is increased and the resonance peaks are spread over a greater range allowing for better resolution. The relatively small ranges for hydrogen result in potential artifacts caused by overlapping images as the selected peaks are so close together.

In vivo CSI has been shown to be useful for several reasons. First, the human body contains a large number of both water and lipid protons. When a hydrogen NMR spectrum for the human body is observed, it consists of major peaks corresponding to water and lipid frequencies. Second, water or lipid protons can be imaged separately or together as a composite image. It should then be possible to form an image from only a selected portion of the

total MR spectrum. Third, spatial distribution of a specific resonance frequency is possible, resulting in quantification data.

2.3.1 Selective Saturation and Excitation, and CSI.

When an appropriate pulse sequence is applied to a specimen, the net magnetization vector is 'tipped' and an MR signal is produced. If the condition were set such that there were no difference in upper and lower nuclear magnetic states, and if additional radio frequency does not cause net transitions to occur between energy states, such a condition would be said to be saturated (Pykett and Rosen, 1983). Such a condition would result in no net magnetization vector and therefore no MR signal from those 'spins' in saturation.

Saturation can be caused by the application of excess radio frequency and is dependent on T1 relaxation time of the resonance of a particular specimen (Bottomley et al., 1984). If a specific resonance peak is saturated immediately before performing a pulse sequence for data acquisition, there is no signal from the saturated peak. One peak can be saturated exclusively and thus its signal negated during the data collection.

Conversely, a particular resonance peak can be selectively excited by the application of an appropriate radio frequency, used to excite a narrow range of resonance frequencies distributed about a particular nuclear frequency. This concept is employed in conventional MRI. For example, a frequency-selective 90° pulse is applied in conjunction with the gradient in

the plane of choice (Haase et al., 1985). The selective pulse contains a defined range of frequencies with which it can excite hydrogen nuclei and when superimposed with the slice defining gradient pulse, spatial mapping is possible. Selective saturation and selective excitation are techniques that are employed to acquire the information necessary for chemical shift imaging.

Pykett and Rosen (1983) imaged cat heads and human forearms in a 1.44 T magnet (8 cm bore) using selective excitation and saturation recovery pulse sequence. This resulted in a conventional MR image, with water and fat spectra available for each voxel. With a 64 X 64 pixel image size, the data acquisition was one hour.

Bottomley et al., (1984) and Rosen, Wedeen & Brady (1984) also used a selective saturation pulse sequence, saturating either water- or fat-protons immediately before applying a conventional spin-echo pulse sequence. This showed that it was possible for in vivo NMR signals to be acquired in a time similar to conventional MRI. Separation of the water and fat images was also demonstrated.

A selective excitation technique known as the Chemical Shift Selective method (CHESS) was described by Haase et al. (1985). The CHESS method incorporated conventional MRI pulse sequences and selective excitation. In this pulse sequence the unwanted NMR signal is selectively excited and then dephased. This allows the desired NMR signal data to be acquired by conventional MRI methods. Excitation of either the water or the fat

resonance by the initial pulse sequence produced a fat or water image respectively, in the same time as conventional MRI. However a combination image is not possible. The CHESS method was demonstrated on human subjects by Frahm et al. (1985). In this study, a 2.0 T whole body scanner image was employed and the first images of human head and hip showed that CHESS imaging was promising for use in clinical investigations.

Joseph (1985) imaged the human forearm using a selective excitation method. In this method, Joseph calculated the optimum pulse length of a selective 180° pulse and derived an equation based on the chemical shift difference between water and fat resonance frequencies. This resulted in a 180° rotation of the desired resonance and a 360° rotation of the unwanted resonance, therefore eliminating its contribution to the signal. This was developed so that either water or fat could be emphasized, which would ultimately lead to images of either water or fat.

2.3.2 Modified Conventional MRI and CSI

Modification of conventional imaging has also been used to image the chemical shift. Sepponen et al. (1984) described a modification of conventional imaging which allowed the acquisition of chemical shift information, corresponding to several chemical shifts, which could then be imaged. The method employed a variable time interval between the 180° pulse and data acquisition, while the time between the 90° pulse and data acquisition was held constant. This was utilized using 16 different time

intervals and resulted in 16 images per slice, each image representing the spectra associated with a particular chemical shift. In essence, it was shown that many spectra could be imaged using conventional imaging technology opening a wide range of research possibilities.

Dixon (1984) reported a method, independent from, but related to the work of Sepponen et al. (1984). In Dixon's method, only two sets of data were collected, which were selected for the resonance characteristics of fat and water. Recognizing the difference between the resonance frequencies of water and fat, it was demonstrated that the NMR signal could be considered a vector sum of the magnetization of the fat protons precessing at one frequency and the water protons precessing at another, higher frequency. Their interaction produced a modulation or beat in time, the position of which was dependent on the relative frequencies of the two signals. In the situation where two maxima overlap, the signal is considered to be in-phase. When one maximum overlaps one minimum, they are said to be opposed, or out-of-phase. Spin-echo data can then be collected for images that are in-phase, also known as water-plus-fat (W+F) images. A second set of data can be collected by setting the 180° radio frequency pulse to acquire data "T/2 earlier" (T=20ms), when the water and fat magnetizations are out of phase, resulting in water-minus-fat (W-F) images. Subsequently, the W+F and W-F images can be added together to produce a water image, or subtracted to render a fat image.

2.3.3 Other CSI Techniques

Several CSI techniques have been published, founded upon the principles of selective excitation, selective saturation and modification of conventional MRI. Ford (1990) presented gradient-amplitude phase-encoded spectral (GRAPES) imaging. This approach is based on modification of conventional MRI and is a variation of the Dixon technique. Similarly, Buxton et al. (1986) used a modification of Dixon's method and demonstrated good quantitative correlation between CSI and true water/lipid content using phantoms. Poon et al. (1989) used a selective saturation pulse sequence to demonstrate the quantification of fat and water and the measurement of differential relaxation time.

2.4 Lipid quantification in Biological tissues using CSI

Lee et al. (1984) and Heiken, Lee & Dixon (1985) applied Dixon's technique in the evaluation of hepatic fatty content. Considering that fatty liver disease was not evident by conventional MRI, the in-phase and opposed data and resulting images contained information sufficient to diagnose fatty liver disease. Lee, Heiken & Dixon (1985) went on to compare this method to conventional spin-echo, inversion-recovery, and computer-assisted tomography images in detecting liver metastases. They showed that opposed images detected more lesions or had higher contrasts in several patients when compared to conventional imaging and CT, and they stated that more

images could be obtained in a given time when compared to inversion recovery.

2.5 Quantification of Adipose Tissue using MRI

Several researchers have described studies which investigate conventional MRI as a possible means of estimating both regional and total body adipose tissue (AT). Preliminary research for the use of MRI as a tool to quantify AT was completed by Foster et al. (1984). Foster et al. (1984) developed a NMR pulse sequence demonstrating the ability to discriminate between high-fat and low-fat tissues.

Pursuant to this, researchers developed methods based on the concept that one could assign a value to AT signal intensity, thus identifying a threshold for AT. This threshold was then used to identify and quantify AT throughout a region or whole body. Subsequently, several researchers (Staten, Totty & Kohrt, 1989; Gerard et al., 1990; Seidell, Bakker & Van der Kooy, 1990; Ross et al. 1991; Roberts et al., 1993; Abate et al., 1994) have published studies in which MRI data was collected and analyzed by assigning AT thresholds which enabled the calculation of AT areas. These areas were then used to calculate AT volumes by multiplying the areas by MRI slice thickness. Multiple slice volumes were added together to determine regional and whole body AT estimates. A related method (Cavalieri) was

demonstrated by Roberts et al. (1993) where tissue volumes were estimated using two-dimensional information.

Some of the initial research involved the comparison of MRI to computer-assisted tomography (CT) (Engstrom et al., 1991; Seidell et al., 1990; Ross et al., 1991). These studies found excellent correlations ($r = 0.98$) and brought to light the ethical and health concerns of radiation exposure associated with CT. Initial research also included animal models and comparison to direct measures of cadavers. Ross et al. (1991) studied AT volumes measured by MRI and CT using rats. Fowler et al. (1992), validated the use of MRI to quantify AT with pigs. In this study, a pig was sacrificed and scanned. The MRI data was compared to direct dissection of the animal which showed that MRI underestimated abdominal percent AT by less than 6 percent.

MRI was also compared with several other established methods. Ross et al., (1992) assessed the relationship between MRI-measured AT and waist-to hip ratio (WHR) and scapula-to-triceps ratio (STR). Staten et al. (1989) showed very high correlations ($r = 0.99$) between MRI-measured subcutaneous AT and intraabdominal AT to estimated total percent body fat measured by hydrostatic weighing. MRI has also been favorably compared to deuterium-oxide dilution ($r = 0.91$) and bioelectrical impedance ($r = 0.92$) methods for determining total body fat (Gerard et al., 1990).

2.6 Lipid Definition and Background

Lipids are water-insoluble organic compounds found in biological systems (Horton et al., 1993). They are generally hydrophobic, but can have amphipathic characteristics. This major class of biomolecules are found in all known living organisms and play an essential role in the maintenance of life. Lipids function as structural components of biological membranes, as intracellular storage depots of metabolic energy, as thermal insulation and padding, and in the synthesis of steroid hormones.

Glycerophospholipids are the most abundant lipid of biological membranes. Other membrane lipids include sphingolipids and steroids. The simplest type of glycerophospholipid, is based on the model of a glycerol-3-P backbone or head which has two fatty acid tails. The head is polar while the tails are non-polar. The membrane is therefore composed of a lipid bilayer with the polar heads on the internal and external surface of the cell membrane and the non-polar tails directed towards the center of the membrane. Sphingolipids are also amphipathic and are found in greatest amounts within the mammalian central nervous system. Steroids constitute a third class of membrane lipids and include cholesterol.

Triglycerides are the simplest and most abundant lipid found in the body. Triglycerides are often referred to as fat and they provide metabolic energy stores for an organism. Like many other lipids, triacylglycerols are

composed of three fatty acids esterified to a glycerol backbone. Triglycerides are excellent sources of energy as they have many hydrogen bonds available for energy production. Being hydrophobic, triacylglycerols are not soluble in water and therefore they can be stored with greater efficiency compared to carbohydrates.

Mammalian steroid hormones have a characteristic cyclic nucleus consisting of four fused carbon rings designated A, B, C, and D. Each steroid differs by the total number of carbon atoms present in the side chain attached to the seventeen carbon nucleus. Cholesterol for example is a 27 carbon molecule therefore having ten carbons attached to the ring nucleus. Other mammalian steroid hormones include; 18 carbon estrogens, 19 carbon androgens, and 21 carbon progestins and adrenal corticosteroids.

2.7 Lipid Quantification in Body Composition

Lipids have been functionally classified as essential or non-essential. Essential lipids are those lipids without which the structures and functions of the body could not exist. Examples of essential lipids include lipids found in cell membranes and nervous tissue. Although triacylglycerols have a physiological role in the body they are considered non-essential lipids. They are the most abundant lipid found within the body and are predominantly stored in adipose tissue. Adipose tissue is most commonly found

subcutaneously and is a connective tissue matrix which is composed mainly of triacylglycerols varying greatly in amount.

2.7.1 Lean-Body Mass vs. Fat-Free Mass

It is evident that there is room for interpretation of the nomenclature of the various lipid sources in the body as they relate to tissues overall and body composition in general. Estimates of fat mass are based on a two-compartment model first conceived by Behnke et al., (1942). In the two compartment model the fat mass included all lipids present in the body. The fat-free mass included everything which remained. Since that time the fat-free mass concept has been made more physiologically meaningful by incorporating into it a specified amount of essential fat and calling it lean body mass (Keys and Brozek, 1953). However, this concept has been criticized due to limited empirical data on how much fat is essential (Martin & Drinkwater, 1991).

Data available in the literature is limited to the work of three investigators. These researchers have directly measured the fat-mass and its distribution in 5 adult cadavers. The essential fat (other than triglyceride) was found to vary considerably with a range of 4.3 to 15.2 percent of the total fat-free mass (See Table 1).

Table 1.

Tissue mass distribution in 5 adult cadavers.

	Mitchell (kg)	Forbes 1 (kg)	Forbes 2 (kg)	Forbes 3 (kg)	Moore (kg)
Adipose Tissue	4.08	4.38	12.48	0.14	1.20
Non-adipose Lipid	4.75	6.08	8.05	2.54	2.61
skin	0.72	0.49	0.94	0.28	0.41
muscle	0.75	1.41	2.78	0.59	0.30
bone	1.80	2.37	2.42	1.04	0.06
residual	1.48	1.81	1.91	0.63	1.84
Total lipid	8.83	10.46	20.53	2.68	3.81
Fat-free mass	61.72	43.34	52.97	59.32	39.59
Non-adipose Lipid/ Fat-free mass	7.70%	14.03%	15.20%	4.28%	6.59%

Note: Adapted from Martin and Drinkwater (1991)

There are only 8 reported dissections of cadavers which have included direct measurement of total body lipid by dissection and organic solvent extraction (Forbes et al. 1953, 1956, Mitchell et al. 1945, Moore et al. 1968, Widdowson et al. 1951) and none of these cadavers were subjected to comparative methods of lipid assessment prior to dissection. Forbes et al. (1953, 1956) report values ranging between 2.22 percent and 9.40 percent intramuscular fat. Hawes & Anderson (1993) have reported a study of the

lipid content of arm and leg musculature in representative sections from 3 cadaver specimens. These results showed a range of 6.70 percent to 7.27 percent. Further, Mendez and Keys (1960), have used organic solvent lipid extraction in determining interstitial lipid quantities in small mammals which demonstrated a range of 0.40 percent to 2.28 percent. These values are lower than reported human values and may differ due to inherent differences, but also may differ in the manner of data acquisition. Mendez and Keys (1960), report that the values for fat "refer to extract of muscles stripped of depot fat and represent cell fat and small amounts of interstitial fat".

CHAPTER THREE

METHODOLOGY

This chapter describes the study population, materials and methods used in the collection of anthropometric, magnetic resonance and lipid extraction data. The chapter concludes by describing experimental design and the statistical analysis.

3.1 Cadaveric Specimens

While cadavers offer an important opportunity to study many aspects of man, including body composition, there are certain limitations which must be observed. Few of the bodies donated to medical research are young and representative of a live and healthy state. In addition, there are many researchers requiring access to cadavers for experiments. In general, non-clinical research has a lower priority and the opportunity for 'selection' is limited. Thus it must be accepted that a specimen will be aged and by definition, of poor health.

Cause of death is also an important consideration in using cadaveric specimens. The observed nutritional status in relation to cause of death may offer useful information to the researcher. Cadavers which appear emaciated may have had a history of chronic illness resulting in disproportional tissue

loss. Adipose tissue is the most unstable tissue followed by muscle and bone respectively (Martin, 1984). It should be recognized that this may be an important limitation when conducting research in body composition. Subjects with an acute cause of death would be preferable to those who died from chronic disease.

3.1.1 Specimen Acceptance

All bodies which were made available and were viable, were accepted into the study. Reasons for a specimen being rejected from this study included: severe emaciation; physical abnormality (eg. missing limb or pre or peri-mortem surgical intervention which prevented proper measurement); and early visceral decomposition.

3.2 Specimens

The subjects were cadaveric specimens obtained from the Body Bequethal Program at the Gross Anatomy Laboratory, Faculty of Medicine at the University of Calgary. These bodies are donated to the University of Calgary Medical school for medical education and medical research. From this program six cadavers were accepted for this research. The bodies were those of five caucasian females and one caucasian male. The age ranged from 81 to 97 years.

Four of the subjects were certified as having died due to atherosclerotic cardiovascular disease. This broad term includes such diseases as ischemic

heart disease, thoracic aneurysm and vascular lesions in the brain. One subject died from acute myelogenous leukemia, a bone marrow cancer. Lastly, one subject died of an pneumonia. There were no activity records available on any of the subjects and no further investigation was carried out as to lifestyle prior to death. An expert subjective observation was used to classify each specimen as emaciated, normal, or obese. This classification was used to describe each specimen's overall appearance, giving some insight into the general physical condition of the specimen. (Table 2).

Table 2

Specimen demographics (n=6)

Specimen Number	Age	Gender	Body Appearance	Cause of Death
1	87	F	Normal	ASCVD
2	80	F	Obese	ASCVD
3	97	F	Emaciated	ASCVD
4	88	F	Normal	AML
5	81	M	Normal	Pneumonia
6	91	F	Obese	ASCVD

Note: ASCVD = Atherosclerotic Cardiovascular Disease; AML = Acute Myelogenous Leukemia

All the bodies arrived at the Gross Anatomy Laboratory directly from accredited medical institutions, were assigned an identification number and stored at four degrees Celsius until utilized.

3.3 General Overview of Method

Specimens were removed from the coolers in the Gross Anatomy Laboratory and allowed to warm to room temperature before measurement. With two researchers present, 29 regional and whole body anthropometric measurements were taken and recorded. Immediately following this procedure the right arm and right leg were dissected at the shoulder and hip. The identification number was clearly and permanently marked on the arm and leg. The limbs were individually wrapped in plastic and hung in a walk-in freezer.

Prior to magnetic resonance data collection, the limbs were removed from the freezer and two centimeter thick sections were cut using a pathological bandsaw at the sites representing maximum arm girth, maximum forearm girth, mid-thigh girth and maximum calf girth. These four sections were weighed and then vacuum sealed in plastic bags and allowed to thaw overnight under refrigeration.

The following day, the cut sections were transported to the Magnetic Resonance Imaging Centre at the Foothills Hospital, Calgary, Alberta. Magnetic resonance data were collected and stored on computer hard disc.

This information was transferred to a hard disc drive in the Human Performance Laboratory, University of Calgary and was backed up on tape. Direct subcutaneous adipose tissue (AT) thickness measurements were taken with a pathological ruler on the cut anterior, posterior, lateral and medial surfaces of each segment. Measurements were made from the fascial boundary to the base of the dermal layer of the skin. Segments were dissected into discrete tissues representing adipose tissue, muscle, skin, and bone. The tissue weights were measured and recorded, and later compared to the total section weight which had been previously recorded. The muscle tissue from each section was homogenized in a tissue grinder and stored under refrigeration in an air tight container.

Lipid content of the muscle samples was determined by randomly selecting six one gram samples from the homogenized muscle tissue. Each one gram sample was mixed with methanol and chloroform and the entire mixture was allowed to stand overnight under refrigeration. The mixture was then filtered and washed leaving a mixture of the organic solvents and any extractable lipids. The chloroform and methanol were dried off in a vacuum oven leaving a residue of dissolved lipid. The lipid mass was expressed as a proportion of the original sample.

MR data were analyzed on a Sun computer using a combination of in-house and commercial programs. The data were phase corrected to remove field inhomogeneities. A region of interest was then selected and

information regarding the amount of fat signal present in the data was obtained.

3.4 Specific Procedures

3.4.1 Anthropometric Procedures

Each cadaver was received at the Gross Anatomy Laboratory usually 24-48 hours post-mortem, and was immediately tagged with a number that was recorded along with all pertinent background data, including a brief medical history. Each body was accompanied by documentation issued from the Alberta Justice Department allowing dissection of human remains in the province of Alberta. Each body was then placed in the storage refrigerator and stored at 4°C until the time of measurement.

The day upon which a body was to be measured, the body was removed from the storage area and placed on a stainless steel autopsy table and allowed to warm up to room temperature (20°C). This provided the best conditions for a realistic measurement of the subcutaneous adipose tissue. This took approximately 8 hours.

During measurement the body was supine on an autopsy table for all measurements except for the subscapular skinfold thickness measurement. For this measurement the body was propped on its left side and steadied by a second researcher. A total of 29 girth, breath, skinfold, and length measurements (see Table 3; Appendix A) were taken unilaterally on the right

Table 3

Sites for measurement of girths, breadths and skinfolds.

Girths	Breadths	Skinfolds
Maximal Arm	Biepicondylar humerus	Cheek
Maximal Forearm	Bistylodius	Chin
Mid-Thigh	Biepicondylar femoral	Chest 1
Maximal Calf	Bimalleolar	Chest (axillia)
		Axilla
		Iliocristale
		Suprailium
		Abdomen 1
		Abdomen 2
		Mid-thigh
		Patella
		Medial Calf
		Proximal Calf
		Mid-calf
		Biceps
		Forearm 1
		Forearm 2
		Triceps
		Subscapular

side of the body. All measurements were repeated twice. In the event that the difference between the duplicate measurements was greater than five percent a third measurement was taken and the mean of the two closest measurements was recorded.

There is no accepted protocol for morbid anthropometry, therefore complete details of all the techniques, landmarks and measurement locations are given in Table 3 and Appendix A. These measurements are based on the corresponding *in vivo* landmarks and techniques.

3.4.2 Regional Site Landmarks

Four key measurement sites were landmarked with a permanent felt tipped marker. These marks included the anterior, posterior, lateral and medial aspects of the; maximum upper arm girth, maximum forearm girth, mid-thigh girth, and maximum calf girth.

3.5 Equipment

Equipment for anthropometric measurement included Harpenden skinfold calipers, a Siber-Hegner anthropometer and a Lufkin Executive-Thinline steel band tape measure.

3.6 Sample Preparation

Following the anthropometric measurements, the right arm and right leg were dissected from the body. The arm was dissected at the shoulder and did not involve any cutting of bone. An incision was made lateral to the acromion process and passed antero-medially to the axilla. The incision continued along this same line through the axilla and then proceeded

postero-laterally to the starting point, thus circumscribing the shoulder joint at an approximate angle of 45° in the sagittal plane. The dissection resulted in the head of the humerus being exposed. The capsule, ligaments and tendons were dissected appropriately to remove the arm in its entirety. A similar procedure was followed for removal of the right leg. The leg incision began on the lateral surface of the thigh several centimetres superior to the trochanterion, with the incision following the inguinal crease and passing inferior to the gluteal muscles.

The specimens were double-wrapped in polyethylene and tightly closed with packing tape. A light ligature was tied around the wrist and ankle of the respective specimens and hung in a freezer for storage until all six specimens were procured.

Four days prior to MR data collection, the limbs were removed from the storage freezer, unwrapped and two centimeter thick cross-section segments were cut at the four regional landmark sites using a pathological bandsaw. Segments were cut one centimetre proximal and distal to the regional landmark. Finally, the segments were dissected into four discrete tissues of bone, muscle, skin and adipose tissue. Vascular tissue and nervous tissue were not separated from adipose or muscle tissue; these were simply included with the adipose or muscle tissue in which they naturally occurred. Thus any adipose tissue surrounding the vessels and nerves in muscle tissue or adipose tissue underneath the facial boundary of the muscle was included

in the muscle tissue. Each discrete tissue was weighed and placed in separate air tight containers and immediately stored at -20 °C.

3.7 Magnetic Resonance Data Collection

The day before each MR data collection session an appropriate number, approximately 10, muscle specimens were removed from frozen storage and thawed at 4-6 °C overnight. The thawed muscle tissue was transported to the Magnetic Resonance Imaging Centre at Foothill Hospital, Calgary, Alberta, where MR data was collected.

The muscle tissue, in an air tight container, was placed on a plastic tray and held firmly in a vertical position similar to a limb segment in a supine position. Supports were placed on either side of the specimen and adjustments were made to raise the specimen into a position in the frontal plane. This ensured that proper signal strength could be obtained from the entire section and that the specimen was properly aligned in the field of view. Correct positioning was checked by rolling the table into the MR bore and landmarking the specimen with respect to the isocentre of the imaging planes. Attention was given to align the marked anterior and lateral aspects of the specimen in such a way that the section was in a position which represented the supine position of the extremities of an *in vivo* subject. With the specimen correctly positioned, a 12 centimetre surface coil was placed in the frontal plane and secured with tape to the top of the supports.

The entire imager table was automatically rolled into the correct position within the tube for imaging (Figure 1).

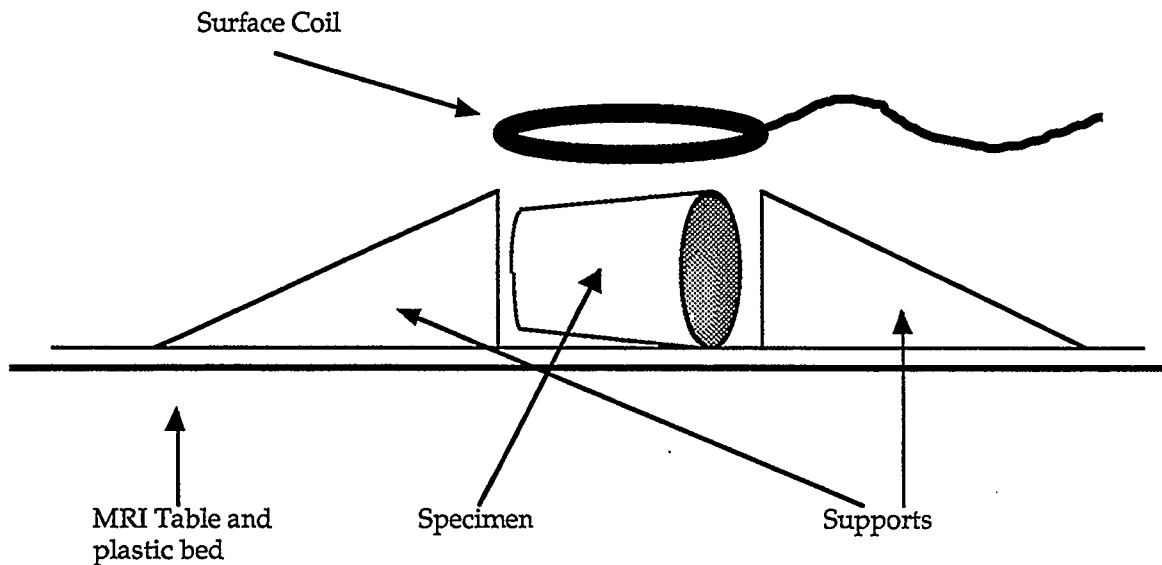


Figure 1. Schematic drawing of specimen set-up on MRI table.

MR data were collected with a Signa 1.5 Tesla whole body scanner (General Electric Medical Systems, Milwaukee, Wisc.). A modified Dixon pulse sequence with a 500-ms repetition time and 20-ms echo time was used for all acquisitions. The number of excitations was two resulting in a scan time of four minutes and ten seconds. All images were acquired on a 256x256 matrix within a 24-cm field of view giving 0.94-mm pixels. One 20 mm transverse slice was imaged per specimen.

File information was written directly to the MR computer hard drive. The raw data were immediately transferred using standard UNIX file transfer protocol to Sun computers in the Human Performance Laboratory.

3.8 Magnetic Resonance Data Analysis

Raw data files were split into water plus fat (W+F) files and water minus fat (W-F) files and were subsequently reformatted from signa images to float images by in house programming. At this point each raw data file was phase corrected using an executable file, (McGibney, 1992), which corrects phase inhomogeneities caused by defective B_0 magnetic field strength, as well as performing an inverse fast fourier transformation (IFFT).

Files were loaded into a software program called Viewdiff (Chow and Smith, 1994) in groups of two. The first file loaded for a given body segment was the real part of the W-F image. This was paired with the real part of the W+F image. With these images loaded the image scale was manipulated to allow the researcher to view the entire image since some portion of the image may be invisible due to poor signal intensity. The W+F and the W-F images were then subtracted, and an image containing 2 times the fat (2F) signal was created. The total signal intensity (W+F) was quantified using the mean square of the image energy. This value represented a mean of the magnitude of the total RF signal vectors for the water plus fat image. Next, the 2F signal intensity was quantified in the same manner but was halved to represent the

fat signal. Finally, the signal representing fat was expressed as a percentage of the total signal. Figure 2 provides a flowchart on the sequence of analysis of magnetic resonance data.

3.9 Lipid Extraction

Six samples were randomly selected from each of the four anatomical regions from each body. Each sample was measured to nominally 1 gram and placed in an air tight container and frozen at -20°C overnight. Individual samples were homogenized with 10 ml methanol (BDH Inc., Toronto, Ont.) and 20 ml chloroform (BDH Inc., Toronto, Ont.) for approximately 2 minutes. This mixture was transferred into clean 70 ml Pyrex (Coring, N.Y.) screw-cap test tubes of a known mass and let stand refrigerated overnight. The liquid and non-liquid material was separated by vacuum filtration. A small amount of chloroform was used to rinse each test tube of all non-liquid material. The liquid material was then replaced in the tube and washed with 7.5 ml of a potassium chloride (BDH, Toronto, Ont.) solution (0.88%). The top layer was aspirated with a micro pipette and the remainder was washed again using a volume of 1:1 v/v solution of distilled water-methanol amounting to more or less one quarter of the volume which remained after the first washing.

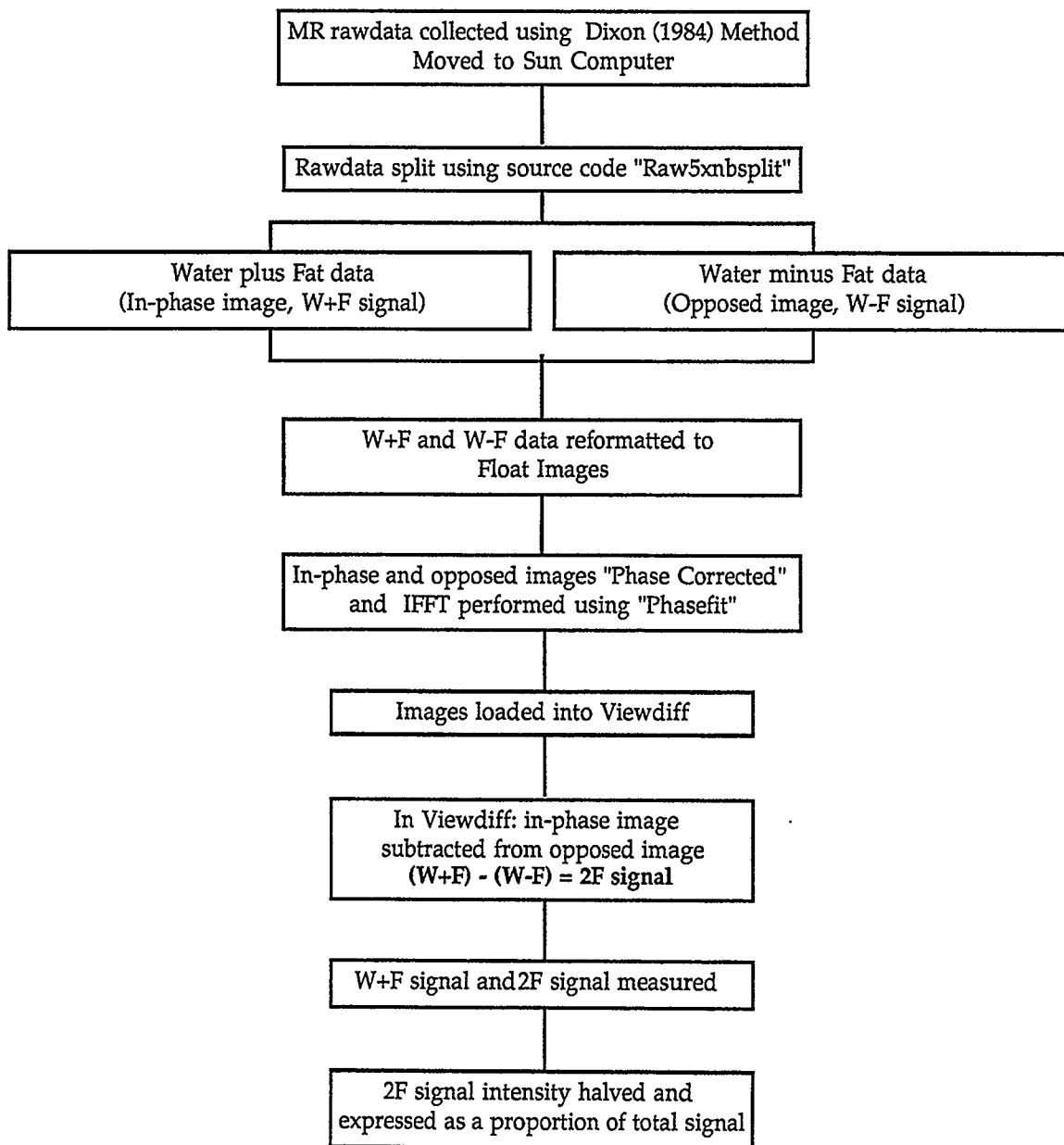


Figure 2. Flowchart of magnetic resonance data analysis.

The top layer was aspirated by micro-pipette. The organic solvents were driven off in a vacuum oven (National Appliance, Portland, Oregon), with the lipid remaining. The test tube and remaining contents (lipid) were reweighed and the lipid content of the sample calculated by the difference for the two measurements and was recorded as a percentage of the initial sample mass. Figure 3 provides a flowchart on the sequence of organic solvent LE methodology.

3.10 Statistical Analysis

Descriptive statistics were calculated and a students t-test performed. The Bland and Altman (1986) method for determining agreement between two measurement techniques was also used. The Bland and Altman (1986) method was developed to offer appropriate analysis of a comparison of a new measurement technique with an established technique. This statistical test compares the difference between the two methods versus the mean of the two methods. Limits of agreement and 95% confidence intervals were calculated. Linear correlations were conducted between values representing muscle tissue lipid content as derived by CSI (dependent variable) and the following independent variables: total body percent fat (Jackson and Pollock, 1978; Jackson et al., 1980) and direct measurement of subcutaneous AT.

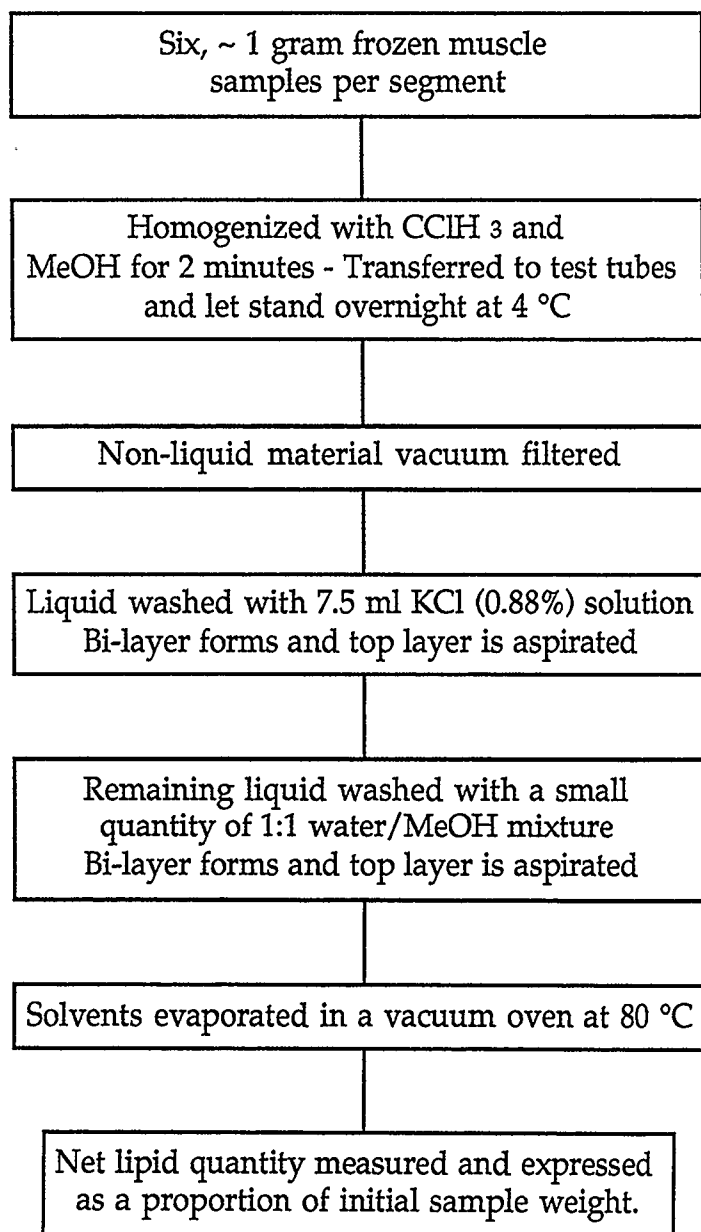


Figure 3. Flowchart of the lipid extraction methodology.

CHAPTER FOUR

RESULTS

This chapter presents descriptive statistics for the anthropometric data, body composition calculations, data from chemical shift imaging and lipid extraction. The comparison of the two methods was analyzed using two statistical interventions. These included a students t-test and the Bland and Altman (1986) method. Correlations between the experimental data and regional and whole body adiposity were conducted. The statistical calculations were made using Microsoft Excel (Microsoft, 1995).

4.1 Anthropometry

4.1.1 Adiposity

Whole body adiposity was examined using several methods as there are no currently accepted post-mortem body composition methodologies. The Jackson & Pollock (1978) 7 sites and 3 sites (male) and Jackson, Pollock & Ward (1980) 7 sites and 3 sites (female) methods were used along with the Parizkova (1978) 10 site method. Sum of skinfolds and estimated percent body fat are outlined in Table 4 and Appendix B.

Table 4

Specimen adiposity estimates.¹

Specimen:	1	2	3	4	5	6
Gender:	(F)	(F)	(F)	(F)	(M)	(F)
Sum of Skinfolds	(mm)	(mm)	(mm)	(mm)	(mm)	(mm)
Parizkova(10)	115.0	374.5	84.5	123.0	61.1	310.8
J and P (7)	94.6	283.4	54.8	89.6	40.6	259.4
J and P (3)	51.2	114.2	24.2	36.6	16.4	106.2
Percent Body Fat						
Parizkova (10)	20.30	40.59	15.00	21.45	10.86	37.38
J and P (7)	23.04	45.69	16.76	22.27	11.80	44.42
J and P (3)	24.82	42.59	15.56	19.68	10.29	41.44
Sample SD between methods	2.28	2.57	0.90	1.32	0.76	3.53

Note: ¹ Using Jackson & Pollock (1978) 7 site and 3 site (male), Jackson, Pollock & Ward (1980) 7 sites and 3 sites (female) and Parizkova (1978) 10 sites methods.
J and P = gender specific methods developed by either Jackson & Pollock (1978) and Jackson, Pollock & Ward (1980). See Appendix B. (n=6)

Table 4 shows that the specimens had comparable values describing adiposity across methods. The range of sum of skinfold values among all specimens based on the Parizkova ten site method was 61.1 mm (specimen 5) to 374.5 mm (specimen 2). Similar rank order results were observed when the other methods were taken into account. For example, upon considering methods described by Jackson & Pollock (1978) or Jackson et al. (1980),

specimen 5 possessed the greatest values while specimen 2 possessed the lowest values. Therefore, from the sum of skinfold data, a trend dividing the specimens into two groups was observed. Specimens 1,3,4 and 5 had a range of 61.1 mm to 123.0 mm, (which might be considered very close to normal), while specimens 2 and 6 had values which ranged from 310.8 mm to 374.5 mm (considered obese).

The values representing percent fat using the Parizkova (1978) method ranged from 10.86 percent (specimen 5) to 40.59 percent (specimen 2). When the other methods were examined the results concurred with those obtained using Parizkova's (1978) ten site method and followed the trend noted across all methods in the sum of skinfold data.

4.1.2 Direct AT Measures

Values representing the sum of four (anterior, posterior, lateral, and medial) direct AT measures for each segment are found in Table 5.

4.1.3 Muscle Mass

Values for estimation of muscle mass using the equation developed by Martin et al. (1990) and Matiegka (1921) can be found in Table 6. Although the equation developed by Martin et al. (1990) precludes its use for female population due to a lack of validation, it was deemed that the Martin et al. (1990) method offered a reasonable estimate, in light of the lack of an alternative method validated with cadavers.

Table 5

Sum of four (anterior, posterior, lateral and medial) direct AT measurements.

Specimen Number:	1	2	3	4	5	6
Gender:	(F)	(F)	(F)	(F)	(M)	(F)
Direct AT Measure: (Σ of 4 Measures - mm)						
Upper Arm:	61	102	29	52	0	72
Forearm:	12	51	18	29	2	31
Upper Leg:	89	72	31	82	15	76
Lower Leg:	56	47	25	31	5	29
Total:	218	272	103	194	22	208

The range using Martin's (1990) equation was 31.6 percent to 45.1 percent and by Matiegka's (1921) method the values fall between 23.3 and 39.2 percent.

Table 6

Estimation of specimen muscle mass. ¹

Specimen Number:	1	2	3	4	5	6
Gender:	(F)	(F)	(F)	(F)	(M)	(F)
Muscle Mass: (%)						
Matiegka (1921):	33.7	23.3	27.0	26.2	39.2	29.2
Martin (1990):	45.1	33.7	31.6	33.6	45.0	35.3

Note: ¹ Using methods described by Matiegka (1921) and Martin (1990). See Appendix B. (n=6)

4.1.4 Skeletal Mass Estimation

Skeletal mass was estimated using two methods. These included methods described by Matiegka (1921) and Drinkwater (1986). The values obtained using these methods are displayed in Table 7. Rawdata and calculations are presented in Appendix B. These values illustrate a consistent skeletal robustness amongst all six specimens of the sample population. When viewed between methods, the results offer no conflicting information.

Table 7

Estimation of specimen skeletal mass. ¹

Specimen Number:	1	2	3	4	5	6
Gender:	(F)	(F)	(F)	(F)	(M)	(F)
Skeletal Mass: (kg)						
Matiegka (1921):	8.31	8.34	7.91	8.26	9.98	8.13
Drinkwater (1986):	6.37	6.39	6.06	11.4	7.65	6.23

Note: ¹ Using methods described by Matiegka (1921) and Drinkwater (1986). See Appendix B.

4.2 Comparison of Methods for Lipid Estimate

4.2.1 Descriptive Analysis

Values which represent the quantified lipid found within the dissected muscle tissues are shown in Table 8. Rawdata and calculations are presented in Appendix B. The presentation includes a comparison between the experimental and comparative methods. These values are presented by segment and by specimen and they include a mean percent lipid value for each specimen.

The values for measured lipid content in skeletal muscle within the study population were homogeneous between methods for specimen one, two and three. The greatest difference in magnitude between methods in specimen 1 was 1.95 percent. In specimen two and three the greatest magnitude difference was 4.41 percent and 4.61 percent respectively. The remaining difference values were less than two percent for these specimens.

Table 8

Comparison of percent lipid using CSI and LE methods.

Specimen:	1			2		
Method:	CSI	LE	(DIFF)	CSI	LE	(DIFF)
Segment	(%)	(%)	(%)	(%)	(%)	(%)
Upper Arm:	6.50	5.05	(1.45)	12.82	13.88	(-1.06)
Forearm:	4.13	5.64	(-1.51)	15.96	16.26	(-0.30)
Upper Leg:	2.50	4.45	(-1.95)	13.44	9.03	(4.41)
Lower Leg:	4.33	5.11	(-0.77)	16.06	15.92	(0.14)
Mean (sd):	4.36 (1.65)	5.06 (0.47)		14.57 (1.68)	13.77 (3.33)	
Specimen:	3			4		
Method:	CSI	LE	(DIFF)	CSI	LE	(DIFF)
Segment:	(%)	(%)	(%)	(%)	(%)	(%)
Upper Arm:	8.93	7.68	(1.25)	5.35	9.58	(-4.23)
Forearm:	12.97	11.91	(1.01)	3.84	5.54	(-1.70)
Upper Leg:	19.29	17.87	(1.42)	17.89	5.68	(12.21)
Lower Leg:	18.85	14.24	(4.61)	6.51	4.71	(1.80)
Mean (sd):	15.01 (4.97)	12.93 (4.27)		8.40 (6.42)	6.38 (2.17)	
Specimen:	5			6		
Method:	CSI	LE	(DIFF)	CSI	LE	(DIFF)
Segment:	(%)	(%)	(%)	(%)	(%)	(%)
Upper Arm:	4.13	6.67	(-2.53)	9.29	13.31	(-4.02)
Forearm:	15.02	8.03	(6.98)	4.73	10.50	(-5.77)
Upper Leg:	7.19	6.40	(0.79)	4.68	14.48	(-9.80)
Lower Leg:	7.35	8.66	(-1.38)	3.02	13.40	(-10.38)
Mean (sd):	8.42 (4.64)	7.44 (1.08)		5.43 (2.70)	12.89 (1.70)	

Note: CSI = chemical shift imaging (n=24); LE = lipid extraction (n=144); DIFF = (CSI-LE)

Difference (magnitude) values of 6.98 percent and 5.77 percent are observed in the forearm segments of specimen five and specimen six. These represent differences which are nearly two fold greater than the lower value. In the fourth specimen the CSI value for the upper leg is over three fold greater than the value obtained using LE. The values observed in the leg segments of specimen six are three fold greater than the CSI values.

The observed values for percent lipid among segments within a specimen show that the greatest range is found in specimen four using the CSI method, 17.89 percent to 3.84 percent (14.04 %). The lowest range is 5.64 percent to 4.45 percent (1.19 %), found using the LE method in specimen one.

4.2.2 Assessment of Agreement

The method of Bland and Altman (1986) offers an evaluation of the agreement between two estimates of the same parameter. This statistical technique was recommended for the investigation of any possible relationships between the measurement error and the mean muscle lipid content in a given segment. This approach questions the accuracy of both estimates with regard to the true mean which is then estimated by the mean of the two measurement techniques.

The newer estimation procedure for lipid content (CSI) was subsequently evaluated against an established procedure (LE). Figure 4 is a Bland and Altman plot of the data where the x-axis displays the mean of the two methods and the y-axis plots the difference between methods.

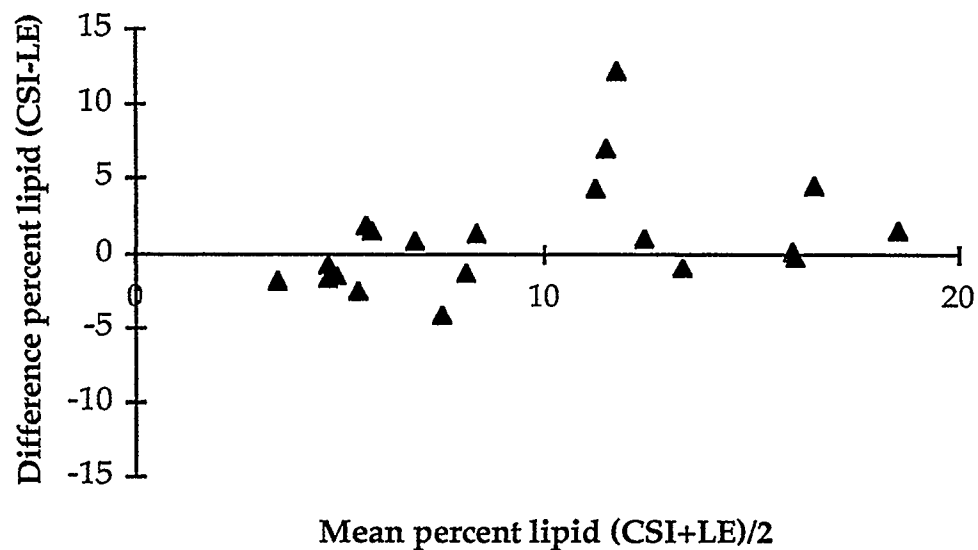


Figure 4 Difference of percent lipid (CSI - LE) against mean percent lipid (CSI + LE)/2.

The plot in figure 4 suggested agreement between methods due to the proximity of the data points to the x-axis, with only two data points having a magnitude greater than five percent difference. Further, agreement was depicted by the ovaloid distribution of the data, with its long axis parallel to the x-axis with a non-significant slope coefficient as indicated by the 95 percent confidence interval (-2.35 to 1.59).

The limits of agreement were calculated using the mean plus or minus 2 times the standard deviation. The calculated values range from 9.27 to -10.04 and include zero. Therefore, the analysis of the data suggested that the methods were in agreement, however this range was a conservative estimate,

(mean plus or minus 2 times standard deviation) of the extreme differences which may be observed between the methods in a similar population. A 95 percent confidence interval was calculated with values ranging between 1.59 to -2.35 which indicates similar information to the limits of agreement while taking the small sample size into account.

4.2.3 Paired student's t-test

The mean difference and standard deviations between estimates was -0.38 (± 4.83) percent (CSI minus LE). A paired students t-test suggested that the difference between the mean percent lipid estimated in cadaveric muscle tissue as determined by CSI or extracted by organic solvents was not significant ($t_{(23)} = -0.39$) $p = 0.35$.

4.2.4 Correlation

Values representing estimates for CSI measured, individual segment, muscle tissue lipid content correlated poorly ($r=0.14$) with direct measures of AT of regional sites. However, there was a moderate correlation ($r=0.58$) between mean values of lipid content of muscle tissue for an individual specimen and total body percent fat as calculated by Jackson & Pollock (1978) and Jackson et al. (1980) (seven site method for males and females).

CHAPTER FIVE

DISCUSSION

In this study an attempt was made to validate a particular chemical shift imaging protocol used to quantify lipid in biological tissue against an established method of lipid quantification. No attempt was made to demonstrate the individual scientific strength of each method as this has been reported previously (Bottomley, Foster, & Leue, 1984b; Dixon, 1984; Lee et al., 1984; Wong, 1994), however, an explanation of the use of the method will be offered in this chapter. By comparing CSI and organic solvent LE, it has been demonstrated that values obtained by CSI do not differ significantly from those obtained by organic solvent LE. An investigation of the relationship between CSI derived lipid content of cadaveric muscle tissue and anthropometric measures of adiposity showed poor correlations with direct (local) measures and moderate correlations with estimated total body percent fat.

5.1 Magnetic Resonance Imaging Methods

The use of MR based methodology to quantify AT in the human body has been well documented and shown to correlate with other imaging techniques, such as computer tomography (CT) (Engstrom et al., 1991; Seidell

et al., 1990; Ross et al., 1991) and various anthropometric measures (Staten et al., 1989; Abate et al., 1994). MRI has the advantage over these methods in that CT involves ionizing radiation which precludes its use over any significant length of time. However, while the positive contribution of MRI to human body composition measurement has been documented to be significant, its exact role has not been defined.

5.1.1 Conventional MRI

Methods which use conventional MRI to measure AT have been outlined previously in the review of literature. Ross et al. (1991), used a conventional MRI protocol to “firmly establish a model that uses MRI to measure AT volume”, and which is representative of several other MRI methods reported in the literature (Staten et al., 1989; Ross et al., 1992; Gerard et al., 1991; Fowler et al., 1990; Seidell et al. 1990; Abate et al., 1994; Roberts et al. 1993). In these studies the approach taken was to obtain MR images with bright pixel intensity for AT. A threshold value was assigned to AT by determining signal strength of regions known to contain AT. Interactive computer programs were employed to determine the number of pixels which were above threshold and areas were calculated based on known pixel areas. In these studies, the calculation of AT area and subsequent AT volume were measured at the anatomical level. Although MRI offers a method of measuring certain body composition parameters in a pseudodirect manner, the validity of these methods are limited. Only one study has compared

results with human cadavers (Abate et al., 1994). In this study MR images were acquired on three cadavers and AT volumes were calculated for three AT regions described as subcutaneous, intraperitoneal and retroperitoneal. AT from these regions was dissected and measured directly. The results of Abate et al. (1994) showed that the MRI measurements compared well to direct measurement, with a slight overestimation of AT mass using MRI.

These methods have limitations in their precision. Stark et al. (1983) experimentally induced fatty liver disease in rats and demonstrated that conventional MR imaging was insensitive in detecting fatty infiltration. It was demonstrated that pixel intensity increased only minimally despite massive increases in triglyceride content. Lee et al. (1984) reported similar results using human subjects with known hepatic fatty infiltration (CT determined) as compared to normal human subjects. The apparent lack of sensitivity may be explained by low relative values of lipid within a given tissue and the uniform distribution of the lipid throughout the tissue. For example, given that normal liver contains five percent fat by weight (Alpers & Isselbacher, 1975) and that this fat is uniformly distributed (Lee et al., 1983), the signal intensity for any given pixel could not be considered at or above a threshold set for fat. Therefore, although the lipid within a given tissue contributes to the signal of each pixel, no one pixel reaches the threshold intensity considered (i.e. above 50%). Roberts et al. (1993) summarized the relevance of this limitation by stating "In future studies fat or water

suppression imaging techniques could be used to remove the chemical shift artifact, which in the present study probably caused a negligible bias in the relevant volume estimates”.

5.1.2 Chemical Shift Imaging

Three general approaches have been forwarded to describe methods of *in vivo* proton CSI. These include selective saturation, selective excitation and modification of conventional MRI. Selective saturation based methods used on the proton chemical shift were reported initially by Pykett and Rosen, (1983) and were followed by other related methods (Bottomley et al, 1984; Rosen et al., 1984). Selective excitation methods were outlined by Haase et al., (1985) and Joseph (1985). A possible limitation of these methods was the inability to collect data as a single image containing both water and methylene data. Dixon & Lee, (1985) commented on the importance of single image data acquisition by suggesting that a single opposed image provides spectroscopic information not available in conventional images and anatomical clarity absent in separated images.

5.2 Agreement of Methods

5.2.1 Descriptive Data

The descriptive analysis of the comparison of percent lipid as determined by CSI and by LE showed that the values measured were generally consistent between segments within a given specimen. The exception to this

was specimen 6, where three out of the four values showed at least a two-fold and as high as a four-fold difference when CSI and LE were compared (Table 8). Anthropometric measures of this specimen revealed high values for estimation of adiposity (Table 4). In specimens with high values of adiposity it was noted that AT within the dissected muscle tissue was more abundant compared to leaner specimens. Figure 5 is a reproduction of two photographs representative of the upper leg segment for an obese specimen (top) and a lean specimen (bottom). The arrows in Figure 5 (top) illustrate an example of the AT which was included in the dissected muscle tissue. Thus, the inclusion of the AT associated with the nerves and vessels of the dissected muscle tissue could increase the absolute amount of AT and augment the random chance of measuring samples which had a greater proportion of lipid compared to the dissected tissue as a whole.

Examination of the mean percent lipid content of dissected muscle tissue for each specimen reveals a trend in the data between specimens which is similar to data reported by Hawes, Hudson & Anderson (1994). Hawes et al., (1994) reported remarkably constant values for mean segmental intramuscular lipid (7.26, 6.72, 6.70 and 5.57 percent) using organic solvent LE. Organic solvent LE obtained values reported in the present study show similar values with the exception of two outliers (4.36, 5.42, 8.39, 8.42, 14.57 and 15.01). The two outliers were the two obese specimens. The values

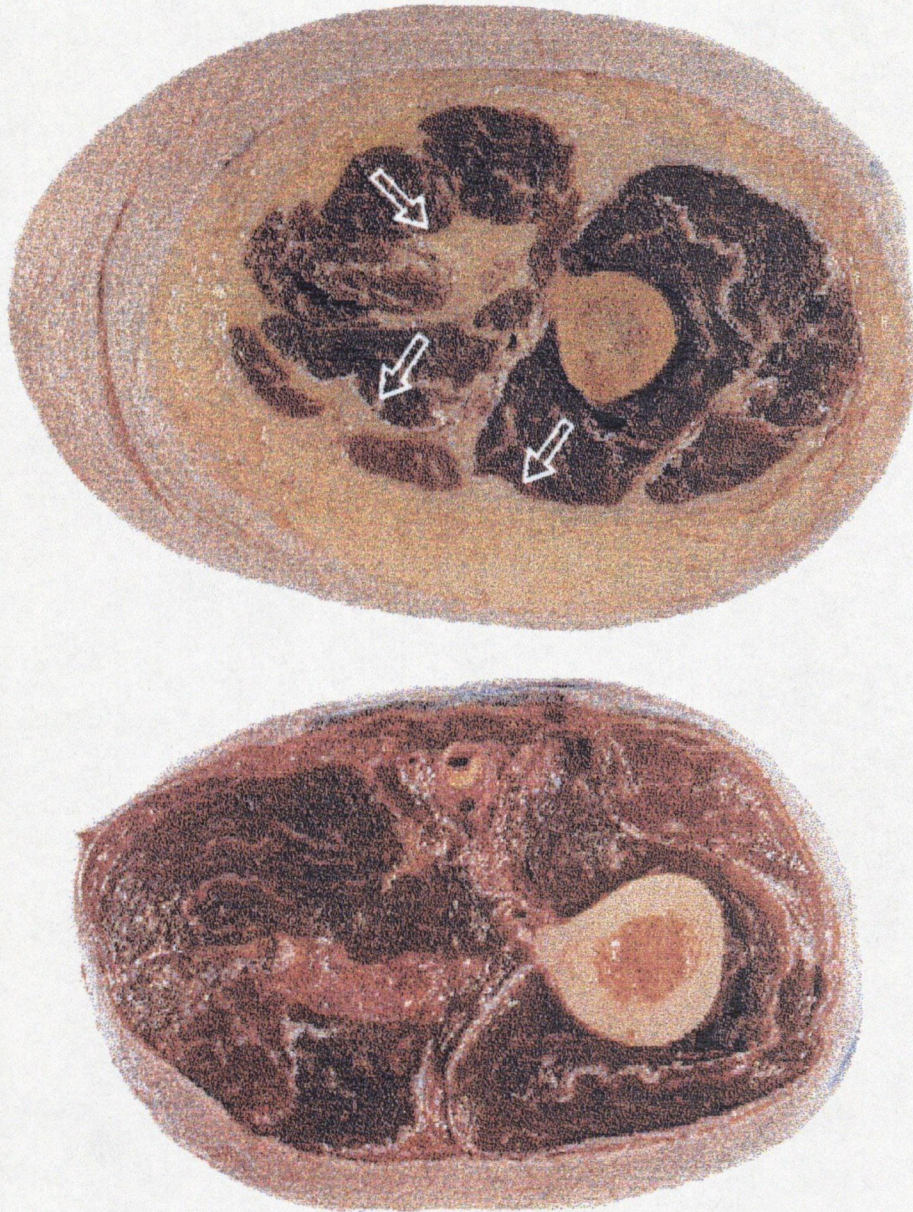


Figure 5. TOP: Photograph of upper leg segment representative of AT distribution in an obese specimen. Arrows indicate AT included in dissected muscle tissue. BOTTOM: Photograph of upper leg segment representative of a lack of subcutaneous and intra-muscular AT in a lean specimen.

reported in the present study differ from those reported in mammalian animal studies. Mendez and Keys, (1960), however, reported values for "the ether extract of muscles stripped of depot fat" which was measured as a percentage by weight and ranged from 0.40 to 1.24 percent for rabbits and 1.08 to 2.28 percent for dogs.

5.2.2 Statistical Procedures

The best statistical approach is not obvious when determining validity of an experimental method. The product-moment correlation coefficient between the results of the two measurement methods is often used as an indicator of agreement. However, such a statistical test only measures the strength of the relationship between two measures and not agreement. Only perfect agreement could be measured in this way ($r=1.0$) (Bland and Altman, 1986).

The control method used in the present study is a direct measurement technique in which lipids are 'dissolved' in organic solvents. The description of the Mangold (1984) method reports lipid recovery in the order of 95 to 99 percent in most animal tissues. Therefore, even as a criterion this method is an imperfect measure of the true value of lipid within the muscle tissue samples. When two such methods are compared neither can provide absolute true values. Bland and Altman (1984) suggest that a mean of two such measures is a better estimate of the true value.

Having an estimated mean calculated for each sample, the means are evaluated for the lack of any systematic error using a linear regression of the difference in estimates as a function of the mean estimate. If a slope coefficient of zero (95 percent confidence interval including zero) is obtained, it indicates agreement (no uncorrectable error) between the estimates and the bias between the estimates can then be evaluated using a students t-test.

The limits of agreement (9.27 to -10.04) and the 95 percent confidence interval (1.59 to -2.35) include zero and were subsequently analyzed using a paired t-test ($t_{(23)} = -0.39$) $p = 0.35$. The results of the t-test confirm the findings of the limits of agreement by suggesting that there is no significant difference between mean lipid content as collected by CSI or organic solvent LE.

The range of the limits of agreement represents the mean difference between the two methods. The range of approximately 9.2 to -10.0 is an indication of the possible mean difference between methods with an extremely conservative outlook. These values indicate that there is a 95.6 percent chance that the true mean lies within these limits. The 95 percent confidence interval (1.5 to -2.3; percent mean difference) indicates that if the same testing procedure were carried out using a similar cadaver population, in 19 out of 20 attempts the mean difference between measures would fall within the stated interval.

While the limits of agreement include zero and therefore suggest agreement, the reported values may be unrealistic in terms of practical use.

The mean values for lipid content reported in Table 8 ranged from 2.5 to 19.3 percent. The limits of agreement (9.2 to -10.0) are practically too large, and may misrepresent the estimated values of lipid content. However, taking into account the sample population size, the 95 percent confidence interval (1.5 to -2.3) represents an acceptable range in relation to practical application of the experimental method.

The descriptive values found in Table 8 indicate that the true mean of lipid content for dissected cadaveric muscle may fall between 2.5 to 19.3 percent. A larger sample size could possibly reduce the 95 percent confidence interval thus narrowing the range of the true lipid content values, adding more confidence to the experimental method. Further, through inspection of the analysis of the limits of agreement, the 95 percent confidence interval and the descriptive data found in Table 8, it could be concluded that there is no systematic over- or under-estimation of lipid content of the muscle samples. Either method may over- or under-estimate lipid content when compared to the other.

5.3 CSI Limitations

There are some limitations in this study. Primarily, the interactive nature of Viewdiff may have introduced bias due to human error. The interactive component of Viewdiff requires the operator to select the region of interest (ROI) to be analyzed. Two possible challenges are present as a

result. The first is that the operator is unable to truly randomize the selection of the ROI. The second is entering the ROI coordinate points incorrectly between the in-phase and opposed images.

As MRI and CSI are essentially based on a two-dimensional coordinate system the resultant field of view (FOV) is rectangular and subsequent analyses are carried out using Cartesian coordinate points. This limited the analysis of the circular images of tissue. During CSI data analysis, it was possible to nearly 'cover' the entire image with the rectangular ROI to be analyzed. However, some of the image was not contained in the ROI and therefore was not included in the analysis. This may be of concern as the tissue at this point was not homogenized. This may have introduced a source of error which cannot be easily corrected.

5.4 Body Composition

Adiposity was measured by using methods of estimation outlined by Parizkova (1978), Jackson & Pollock (1978) and Jackson, Pollock & Ward (1980). Direct measures of subcutaneous adipose tissue were made on the anterior, posterior, lateral and medial aspects of cut segments. These results are shown in Table 4 and 5. These measurements demonstrate a similar rank order. Specimen 1, 3, 4 and 5 had values which could be considered normal, but still representative of a range of body types. For example, specimen 5 was a very lean male with an estimated percent body fat between 10.3 to 11.8

percent. Specimen 1 was a female with an estimate of percent body fat between 20.3 to 24.8 percent. Direct measures of subcutaneous AT were also a valuable indicator of the range of adiposity among specimens. Specimen 5 possessed extremely low values, ranging from 0 to 15 mm. In contrast, the values reported for specimen 2 ranged from 47 to 102 mm.

5.5 Relationships Between Intra- and Extra-cellular Lipid and Other Fat Depots

The secondary purpose of the study was to investigate any possible relationships between the lipid content of dissected cadaveric muscle and estimates of adiposity. The r -values reported in the results, indicate that direct subcutaneous AT measurements did not correlate well with lipid content values ($r = 0.14$). Conversely estimates of total percent body fat (Jackson & Pollock, 1978; Jackson et al., 1980) moderately correlated ($r = 0.58$) with lipid content values. CSI is a measure of lipid at the molecular level while skinfold estimates of total percent body fat are derived from regression to molecular estimates (desitometry) of total fat which are related to a molecular level of the measurement. This may suggest that total percent body fat is a good indicator of the amount of lipid stored in an inter- and intra-muscular fashion. Measures such as the sum of skinfolds, which is an indicator of anatomical subcutaneous AT would not be expected to be indicative of the lipid content of muscle.

5.6 Future Considerations

CSI, as presented in this thesis, has shown potential to be an alternative method for the assessment of human body composition. However, the development of the analytical technology and related computer software must be improved to allow more user friendly environment. This development may include computer software which allows the analysis of circular images and which is dedicated to the analysis of the water/fat chemical shift.

With such advancement, CSI may become a useful tool in the investigation and comparison of other methods which are based on the two compartment models of body composition. Other molecular level related human body composition studies would also benefit. Related to this, CSI may be used in conjunction with anatomical MRI techniques in furthering the investigation of human body composition.

5.7 Conclusion

In conclusion, the results of this study indicate that the values of intra- and extra-cellular lipids found within cadaveric skeletal muscle obtained by the experimental method are similar to those obtained by the control method.

REFERENCES

- Abate, N., Burns, D., Peshock, R.M., Abhimanyu, G. & Grundy, S.M. (1994). Estimation of adipose tissue mass by magnetic resonance imaging: Validation against dissection in human cadavers. *Journal of Lipid Research*. 35: 1490-1496.
- Ackerman, J.J.H., Grove, T.H., Wong, G.G., Gadian, D.G., & Radda, G.K. (1980). Mapping of metabolites in whole animals by ^{31}P NMR using surface coils. *Nature*. 283: 167-170.
- Alger, J.R., Sillerud, L.O., Behar, K.L., Gillies, R.J., Shulman, R.G., Gordon, R.E., Shaw, D. & Hanley, P.E. (1981). *In vivo* carbon-13 nuclear magnetic resonance studies of mammals. *Science*. 214: 660-662.
- Alpers, P.H. & Isselbacher, K.J. (1975). Fatty liver: biochemical and clinical aspects. In: L. Schiff (Ed.), *Diseases of the liver*. (pp. 15-32). Philadelphia: J.B. Lippincott.
- Behnke, A.R. (1942). Physiological studies pertaining to deep sea diving and aviation, especially in relation to the fat content and composition of the body. *Harvey Lectures* (1941-1942): 198-226.
- Bland, J.M. & Altman, D.G. (1986). Statistical methods for assessing agreement between two methods of clinical measurement. *Lancet*. 1: 307-310.

- Borkan, G.A., Hults, D.E., Gerzof, S.G., Burrows B.A. & Robbins, A.H. (1983). Relationships between computed tomography tissue areas, thicknesses and total body composition. *Annals of Human Biology*. 10: 537-46.
- Borkan, G.A., Gerzof, S.G., Robbins, A.H., Hults, D.E., Silbert, C.K., & Silbert, J.E. (1982). Assessment of abdominal fat content by computed tomography. *American Journal of Clinical Nutrition*. 36: 172-77.
- Bottomley, P.A., Foster, T.H. & Leue, T.M. (1984a). *In vivo* nuclear magnetic resonance chemical shift imaging by selective irradiation. *Proceedings. National Academy of Science (United States of America)*. 81: 6856-6860.
- Bottomley, P.A., Foster, T.H. & Leue, T.M. (1984b). Chemical imaging of the brain by NMR. *Lancet*. 1: 1120
- Brown, T.R., Kincaid, B.M. & Ugurbil, K. (1982). NMR chemical shift imaging in three dimensions. *Proceedings. National Academy of Science (United States of America)*. 79: 3523-3526.
- Buxton, R.B., Wismer, G.L., Brady, J.T. & Rosen, B.R. (1986). Quantitative proton chemical-shift imaging. *Magnetic Resonance in Medicine*. 3: 881-890.
- Chow, K. & Smith, M. (1994). *Viewdiff*. [Computer Program].
- Cox S.J. & Styles P. (1980). Towards biochemical imaging. *Journal of Magnetic Resonance*. 40: 209-212.
- Dixon W.T. (1984). Simple proton spectroscopic imaging. *Radiology*. 153: 189-194.

- Drinkwater, D.T., Martin A.D., Ross, W.D. & Clarys, J.P. (1986). Validation by cadaver dissection of Matiegka's equations for the anthropometric estimation of anatomical body composition in adult humans. In: J.A.P. Day (Ed.), *The 1984 Olympic Scientific Congress Proceedings-Perspectives in Kinanthropometry*. (pp. 221-227). Champaign: Human Kinetics.
- Engstrom, C.M, Loeb, G.E., Ried, J.G., Forrest, W.J. & Auruch, L. (1991). Morphology of human thigh muscles. A comparison between anatomical sections and computer tomographic and MR images. *Journal of Anatomy*. 176 : 139-156.
- Folch, J., Lees, M., & Stanley, H.S. (1957). A simple method for the isolation and purification of total lipides from animal tissues. *Journal of Biological Chemistry*. 226: 497-509.
- Forbes, R.M., Cooper, A.R. & Mitchell, H.H. (1953). The composition of the adult human body as determined by chemical analysis. *Journal of Biological Chemistry*. 223: 359-366.
- Forbes, R.M., Mitchell, H.H. & Cooper, A.R. (1956). Further studies on the gross composition of the adult human body. *Journal of Biological Chemistry*. 223: 969-975.
- Ford, J.J. (1990). Gradient-amplitude phase-encoded spectral (GRAPES) imaging. A novel approach to spin-echo chemical shift imaging. *Journal of Magnetic Resonance*. 87: 346-351.

- Foster, M.A., Hutchinson, J.M.S., Mallard, J.R. & Fuller, M. (1984). Nuclear magnetic resonance pulse sequence and discrimination of the high- and low-fat tissues. *Magnetic Resonance Imaging*. 2: 187-192.
- Fowler, P.A., Knight, C.H., Cameron G.G. & Foster, M.A. (1990). Use of magnetic resonance imaging in the study of goat mammary glands *in vivo*. *Journal of Reproductive Fertility*. 89: 359-366.
- Fowler, P.A., Fuller, M. F., Glasbey, C.A., Cameron, G.G. & Foster, M.A. (1992). Validation of the *in vivo* measurement of adipose tissue by magnetic resonance imaging of lean and obese pigs. *American Journal of Clinical Nutrition*. 56; 7-13.
- Frahm, J., Haase, A., Hanicke, W., Matthaei, D., Bomsdorf, H. & Helzel, T. (1985). Chemical shift selective MR imaging using whole-body magnet. *Radiology*. 156: 441-444.
- Gerard, E.L., Snow, R.C., Kennedy, D.N., Frisch, R.E., Guimaraes, A.R., Barbieri, R.L., Sorensen, A.G., Egglin, T.K. & Rosen, B.R. (1991). Overall body fat and regional body fat distribution in young women: Quantification with MR imaging. *American Journal of Roentgenography*. 157: 99-104.
- Gordon, R.E., Hanley, P.E., Shaw, D., Gadian, D.G., Radda, G.K., Styles, P., Bore, P.J. & Chan, L. (1980). Localization of metabolites in animals using ^{31}P topical magnetic resonance. *Nature*. 287: 736-738.

- Haase A., Frahm, J., Hanicke, W. & Matthaei, D. (1985). ^1H NMR chemical shift selective (CHESS) imaging. *Physics in Medicine and Biology*. 30: 341-344.
- Hawes, M.R. & Anderson, P. (1993). Estimated combined muscle and bone volumes by ultrasound and anthropometry validated against cadavers evidence. *Medicine in Science, Sport and Exercise*. 25: 5 (supplement).
- Hawes, M.R., Hudson, S.B. & Anderson, P. (1994). *In vivo* interstitial lipid component of muscle in the extremities. *Proceedings: 10th Commonwealth & Scientific Congress Abstracts*. Victoria, Canada. 1: 202. Abstract no. J1-08-1.
- Heiken, J.P., Lee, J.K.T. & Dixon, W.T. (1985). Fatty infiltration by proton spectroscopic imaging. *Radiology*. 157: 707-710.
- Heymsfield, S.B., McManus, C., Stevens, V. & Smith, J. (1982a). Muscle mass: Reliable indicator of protein-energy malnutrition severity and outcome. *American Journal of Clinical Nutrition*. 35: 1192-1199.
- Heymsfield, S.B., McManus, C., Smith, J., Stevens, V. & Nixon, D.W. (1982b). Anthropometric measurement of muscle mass: Revised equations for calculating bone-free arm muscle area. *American Journal of Clinical Nutrition*. 36: 680-690.

- Heymsfield, S.B., Arteaga, C., McManus, C., Smith, J. & Moffitt, S. (1983). Measurement of muscle mass in humans: Validity of the 24-hour creatinine method. *American Journal of Clinical Nutrition*. 37: 478-494.
- Horton, H.R., Moran, L.A., Ochs, R.S., Rawn, J.D. & Scrimgeour, K.G. (1993). *Principles of Biochemistry*. Englewood Cliffs, N.J.: Prentice Hall. pp. 9.1-9.36.
- Jackson, A.S. & Pollock, M.L. (1978). Generalized equations for predicting body density of men. *British Journal of Nutrition*. 40: 497-504.
- Jackson, A.S., Pollock, M.L. & Ward, A. (1980). Generalized equations for predicting body density of women. *Medicine and Science in Sports and Exercise*. 12: 175-182.
- Joseph, P.M. (1985). A spin echo chemical shift MR imaging technique. *Journal of Computer-Assisted Tomography*. 9: 651-658.
- Keys, A. & Brozek, J. (1953). Body fat in adult man. *Physiology Review*. 33: 245-325.
- Lee, J.K.T., Dixon, W.T., Ling, D., Levitt, R.G. & Murphy, W.A. (1984). Fatty infiltration of the liver: Demonstration by proton spectroscopic imaging. *Radiology*. 153: 195-201.
- Lee, J.K.T., Heiken, J.P. & Dixon, W.T. (1985). Detection of hepatic metastases by proton spectroscopic imaging. *Radiology*. 156: 429-433.

- Lohman, T.G., Roche, A.F. & Martorell, R. (1988). *Anthropometric standardization reference manual*. Champaign: Human Kinetics Books.
- Mangold, H.K. (1984). *Handbook of Chromatography*. Lipids Volume 1. (pp. 36). Boca Raton: CRC Press Inc.
- Martin, A.D. (1984). An anatomical basis for assessing human body composition: Evidence from 25 dissections. *Doctoral Dissertation*, Simon Frazer University, Vancouver.
- Martin, A.D., Spenst, L.F., Drinkwater, D.T. & Clarys, J.P. (1990). Anthropometric estimation of muscle mass in men. *Medicine and Science in Sports and Exercise*. 22: 729-733.
- Martin, A.D. & Drinkwater, D.T. (1991). Variability in the measures of body fat: Assumptions or technique? *Sports Medicine*. 11 (5): 277-288.
- Matiegka, J. (1921). The testing of physical efficiency. *American Journal of Physical Anthropology*. 4: 223-230.
- Matthaei, D., Haase, A., Frahm, J., Schuster, R. & Bomsdorf, H. (1985). Chemical-shift-selective magnetic-resonance imaging of avascular necrosis of the femoral head. *Lancet*. 1: 370-371.
- McGibney, G., (1992) *Phasefit*. [Computer Program].
- Mendez, J. & Keys, A. (1960). Density and composition of mammalian muscle. *Metabolism*. 9: 184-188.

- Mendez, J., Lukaski, .C. & Buskirk, E.R. (1984). Fat-free mass as a function of max. O₂ consumption and 24-hour urinary creatinine, and 3-methylhistadine excretion. *American Journal of Clinical Nutrition*. 39: 710-715.
- Microsoft Corporation (1994). *Microsoft Excel v 5.0*. [Computer Program].
- Mitchell, H.H., Hamilton, T.S., Streggera, F.R. & Bean, H.W. (1945). The chemical composition of the adult human body and its bearing on the biochemistry of growth. *Journal of Biological Chemistry*. 158: 625-637.
- Moore, F.D., Lister, J., Boyden, C.M., Ball, M.R., Sullivan, N. & Dagher, F.J. (1968). The skeleton as a feature of body composition. *Human Biology*. 40: 136-188.
- Oldendorf, W. & Oldendorf, W. (1991). *MRI Primer*. (pp. xi; 17). New York: Raven Press.
- Parizkova, J. (1978). Lean body mass and depot fat during ontogenesis in humans. In Nutrition, Physical Fitness and Health. In: J. Parizkova and V.A. Rogozkin (Eds.), *International Series on Sport Sciences*, 7. (pp. 24-51). Baltimore: University Park Press.
- Poon, C.S., Szumowski, J., Plewes, D.B., Ashby, P. & Henkelman, R.M. (1989). Fat/water quantification and differential relaxation time measurement using chemical shift imaging technique. *Magnetic Resonance Imaging*. 7: 369-382.

- Pykett, I.L., Newhouse, J.H., Buonanno, F.S., Brady, T.J., Goldman, M.R., Kistler, J.P. & Pohost, G.M. (1982). Principles of nuclear magnetic resonance imaging. *Radiology*. 143: 157-168.
- Pykett, I.L. & Rosen, B.R. (1983). Nuclear magnetic resonance: *In vivo* proton chemical shift imaging. *Radiology*. 149: 197-201.
- Roberts, N., Cruz-Orive, M., Reid, M.K., Brodie, D.A., Bourne, M. & Edwards, H.T. (1993). Unbiased estimation of human body composition by the cavalieri method using magnetic resonance imaging. *Journal of Microscopy*. 171:239-253.
- Rosen, B.R., Wedeen V.J. & Brady, T.J. (1984). Selective saturation NMR imaging. *Journal of Computer-Assisted Tomography*. 8: 813-818.
- Ross, R., Leger, L., Guardo, R., DeGuise, J. & Pike, B.G. (1991). Adipose tissue volume measured by magnetic resonance imaging and computerized tomography in rats. *Journal of Applied Physiology*. 70 (5): 2164-2172.
- Ross, R., Leger, L., Morris, D., DeGuise, J. & Guardo, R. (1992). Quantification of adipose tissue by MRI: Relationship with anthropometric variables. *Journal of Applied Physiology*. 72 (2): 787-795.
- Seidell, J.A., Bakker, C.J.G. & Van der Kooy, K. (1990). Imaging technique for measuring adipose tissue distribution: a comparison between computer-assisted tomography and 1.5 T Magnetic resonance imaging. *American Journal of Clinical Nutrition*. 51: 953-957.

- Sepponen, R.E., Sipponen, J.T. & Tantt J.I. (1984). A method for chemical shift imaging: Demonstration of bone marrow involvement with proton chemical shift imaging. *Journal of Computer-Assisted Tomography*. 8: 585-587.
- Siri, W.E. (1956). Body composition from fluid spaces and density: Analysis of methods. *University of California Radiation Laboratory Report UCRL no. 3349*.
- Spent, L.F., Martin, A.D. & Drinkwater, D.T. (1993). Muscle mass of competitive male athletes. *Journal of Sport Sciences*. 11: 3-8.
- Stark, D.D., Bass, N.M., Moss, A.A., Bacon, B.R., McKerrow, J.H., Cann, C.E., Brito, A. & Goldberg, H.I. (1983). Nuclear magnetic resonance imaging of experimentally induced liver disease. *Radiology*. 148: 743-751.
- Staten, M.A., Totty, W.G. & Kohrt, W.M. (1989). Measurement of fat distribution by magnetic resonance imaging. *Investigative Radiology*. 24: 345-349.
- Widdowson, E.M., McCance, R.A. & Spray, C.M. (1951). The chemical composition of the human body. *Clinical Science*. 10: 113-125.
- Wong, W., Northrup, R.S., Herrick, R.C., Glombicki, A.P., Wood, R.P. & Morrisett, J.D. (1994) Quantitation of lipid in biological tissue by chemical shift magnetic resonance imaging. *Magnetic Resonance in Medicine*. 32: 440-46.

APPENDIX A

Anthropometric Measurements

The following includes a detailed description of the landmarks and methods used to obtain anthropometric data describing the cadaveric specimens.

Weight: The body weight estimated using the method outlined in the Anthropometric Standardization Reference Manual (Lohman, Roche, & Martorell, 1988). Measures of arm and calf circumference and subscapular skinfold thickness were used in the following formulae:

Women: Body Weight Estimate = $0.92 (\text{arm circ.}) + 1.50 (\text{calf circ.}) + 0.42 (\text{subscapular skinfold}) - 26.19$

Men: Body Weight Estimate = $1.92 (\text{arm circ.}) + 1.44 (\text{calf circ.}) + 0.25 (\text{subscapular skinfold}) - 39.97$

Height: Recumbent length was measured using an anthropometer. The specimen was placed in a supine position with the buttocks and shoulders flat, knees and hips extended and flat on the table. The stationary end of the device was placed at the heel, and the moving branch was positioned at the crown of the head with the head positioned in the Frankfort Plane. The measurement was recorded to the nearest 0.1 cm.

Girths: Four girth measurements were recorded. The sites of measurement are listed in Table 2 and are described below.

Maximal arm: This measurement was taken with the specimen in a supine position, the arm abducted 90° and allowed to externally rotate to a position of equilibrium. The arm was flexed slightly by a second researcher so as to lift the arm from the table enough to allow the measuring tape to pass freely beneath the arm. The measurement was taken by loosely placing the tape around the arm at approximately the maximal girth and moving the tape superiorly and inferiorly until a maximal measurement was determined. At this level the measurement is recorded to the nearest 0.1 cm and the site is landmarked on all four surfaces with a permanent felt-tipped marker.

Maximal forearm: This measurement was taken with the specimen in the same position as described above. The forearm extended past the side of the table which allowed easy access for measurement. The tape was placed loosely around the forearm at approximately the maximal forearm girth and was then moved superiorly and inferiorly until the level of maximal forearm girth was located. At this level the measurement is recorded to the nearest 0.1 cm and the site was marked on all four surfaces with a permanent felt-tipped marker.

Mid thigh: This measurement was taken with the specimen in a supine position. Initially the body lay flat on the table with the shoulders and buttocks in contact with the table. The leg is also flat on the table. The greater trochanter and head of the fibula are landmarked and half-way distance between these two landmarks is permanently marked on all four surfaces to

represent the mid-point of the thigh. For the girth measurement, the right leg is flexed slightly at the hip and remains in a straight position at the knee. The leg was kept in this position using a block under the heel. The tape was placed loosely around the thigh at the mid thigh mark and the measurement recorded to the nearest 0.1 cm.

Maximal calf: This measurement was taken with the specimen in the same position as described for the mid thigh measurement. The tape was placed around the approximate maximal calf girth and was moved superiorly and inferiorly until the maximum calf girth was determined. At this level the measurement was recorded to the nearest 0.1 cm and the site was landmarked on all four surfaces with a permanent felt-tipped marker.

Breadths: Four breadth measurements were taken. The sites of measurement are listed in Table 2 and are described below.

Biepicondylar humerus (elbow breadth): This measurement was taken with the body in the same position as was described for the maximal arm girth with the exception that the arm was not flexed at the shoulder and was allowed to rest on the table. A second researcher held the forearm vertically by the wrist with the dorsum of the hand facing medially, thus flexing the elbow to approximately 90 deg. The epicondyles of the humerus were palpated and the measurement taken at the greatest distance between the

epicondyles as it would be *in vivo*. The measurement was recorded to the nearest 0.1 cm.

Bistyloidius (wrist breadth): This measurement was taken with the specimen in the same position as described for the maximal arm girth. For this measurement the wrist was pronated. The most medial aspect of the ulnar styloid and most lateral aspect of the radial styloid were palpated and the distance between these two bony prominences was recorded to the nearest 0.1 cm.

Biepicondylar femoral (knee breadth): This measurement was taken with the specimen in the same position as was described for mid-thigh girth. The lateral and medial epicondyles were palpated and the calipers were placed at 90° to the straight knee. A great deal of force was applied to the tissue surrounding the knee so as to attempt to reduce measurement error due to the overlying tissues. *

(* This seemed to only be a concern at the knee as the other joints had very little tissue surrounding them).

Bimalleolar (ankle breadth): This measurement was taken with the specimen in the same position as was described for mid-thigh girth with the exception of the placement of the block to prop the leg up. In this case the block was placed superior to the malleoli to allow unobstructed access. Measurement of the bimalleolar breadth was then completed as it would be *in vivo*.

Skinfolds: Nineteen skinfold measurements were taken. The sites for these measurements are listed in Table 2. All measurements are recorded to the nearest 0.1 mm.

Cheek: Skinfold was taken horizontally below the temple on the line connecting the tragus and the nostrils.

Chin: Skinfold was taken vertically, above the hyoid bone. The neck was slightly flexed but the skin must remain loose.

Chest (pectoral): The skinfold was taken obliquely along the borderline of the pectoralis major between the anterior axillary fold and the nipple. In females, the measurement was taken one-third of this distance, while in men it was taken at one-half the distance.

Chest (axillia): The skinfold was taken horizontally on the chest above the 10th rib at the point of intersection with the anterior axillary line.

Axillia (midaxillary): The skinfold was taken vertically at the level of the xiphoid-sternal junction in the mid-axillary line.

Iliocristale: The skinfold was taken horizontally following the natural cleavage lines of the skin. This skinfold is measured 7 cm superior to the anterior superior iliac spine.

Suprailium: The skinfold was taken obliquely above the crest of the ilium at the spot where an imaginary line would come down from the anterior axillary line.

Abdomen 1 (horizontal): The skinfold was taken horizontally 3 cm lateral and 1 cm inferior to the umbilicus.

Abdomen 2 (vertical): The skinfold was taken vertically at a lateral distance of 2 cm from the umbilicus.

Mid thigh: The skinfold was taken vertically on the anterior aspect of the thigh at the mid-thigh landmark described in measuring the mid-thigh girth.

Patella: With the knee straight, the skinfold was taken vertically in the midsagittal plane 2 cm superior to the proximal edge of the patella.

Medial calf: The skinfold was taken vertically on the medial aspect of the leg at the level of maximum calf girth.

Proximal calf: The skinfold was taken vertically on the posterior aspect of the lower leg in the midsagittal plane 5 cm inferior to the popliteal fossa.

Mid calf: The skinfold was taken vertically on the posterior aspect of the lower leg in the midsagittal plane at the level of maximum calf girth.

Biceps: The skinfold was taken vertically on the midline of the anterior aspect of the arm at the same horizontal level as the triceps skinfold.

Forearm 1 (anterior): The skinfold was taken vertically on the anterior aspect of the forearm at the level of maximum forearm girth.

Forearm 2 (lateral): The skinfold was taken vertically on the lateral aspect of the forearm at the level of maximum forearm girth.

Triceps: The skinfold was taken vertically on the midline of the posterior aspect of the arm exactly half-way between the olecranon process of the ulna and the acromion process of the scapula. This was done by having one researcher roll the specimen on its left side, and while maintaining the specimen in a secure position, flexing the elbow to 90°. A second researcher landmarked the appropriate structures.

Subscapular: The skinfold was taken with the specimen in the same position as described above. The skinfold was taken obliquely 1 cm inferior to the inferior angle of the scapula on the line inclined approximately 45° to the horizontal plane in the natural cleavage lines of the skin.

APPENDIX B

Body Composition Data

Included herein are the raw data and formulas used to estimate muscle mass, percent body fat and skeletal mass for the six specimens.

PERCENT BODY FAT ESTIMATION

Jackson & Pollock (1978) and Jackson, Pollock & Ward (1980) 7 Sites

Specimen Number:	1	2	3	4	5	6
Gender:	(F)	(F)	(F)	(F)	(M)	(F)
Skinfolds (mm):						
Chest 1	11.0	32.4	5.4	16.0	3.0	44.2
Midaxillary	6.6	50.0	12.0	13.6	6.6	45.2
Abdominal 2	17.2	50.0	7.0	14.2	7.4	42.6
Suprailium	12.8	50.0	5.8	11.2	5.8	50.0
Subscapular	8.6	36.8	6.2	9.2	6.2	21.2
Triceps	20.2	20.8	7.4	15.2	5.6	14.6
Mid thigh	18.2	43.4	11.0	10.2	6.0	41.6
Σ of 7 Skinfolds:	94.6	283.4	54.8	89.6	40.6	259.4
Age (yrs.):	87	80	97	88	81	91
Body Density (g/L):	1.046	0.999	1.060	1.048	1.072	1.001
Percent Fat:	23.0	45.7	16.8	22.3	11.8	44.4

Body Density Formulae:

Males = $1.112 - 0.00043499 (\Sigma 7) + 0.00000055 (\Sigma 7)^2 - 0.00028826 (\text{age})$

Females = $1.097 - 0.00046971 (\Sigma 7) + 0.00000056 (\Sigma 7)^2 - 0.00012828 (\text{age})$

Estimation of Percent Body Fat Formula:

Siri = $[(4.95) / \text{Body Density}] - 4.5 \times 100$

Parizkova (1978) 10 Sites

Specimen Number:	1	2	3	4	5	6
Gender:	(F)	(F)	(F)	(F)	(M)	(F)
Skinfolds (mm):						
Cheek	7.0	15.4	6.4	9.2	8.0	13.6
Chin	5.0	24.0	5.8	8.8	4.6	20.2
Chest 1	11.0	32.4	5.4	16.0	3.0	44.2
Chest 2	9.4	50.0	9.8	11.4	8.4	41.2
Iliospinale	10.4	50.0	6.8	11.6	4.1	37.8
Abdominal 1	17.2	50.0	7.0	14.2	7.4	42.6
Subscapular	8.6	36.8	6.2	9.2	6.2	21.2
Triceps	20.2	20.8	7.4	15.2	5.6	14.6
Patella	12.2	45.1	15.2	10.4	5.6	37.0
Proximal calf	14.0	50.0	14.5	17.0	8.2	38.4
Σ of 10 Skinfolds:	115.0	374.5	84.5	123.0	61.1	310.8
Log Σ 10 Skinfolds:	2.061	2.573	1.927	2.090	1.786	2.492
Percent Fat:	20.3	40.6	15.0	21.5	10.9	37.4

Formulae:

Males = $22.32 \log \Sigma 10 - 29.00$ Females = $39.572 \log \Sigma 10 - 61.25$

Jackson & Pollock (1978) and Jackson, Pollock & Ward (1980) 3 Sites

Specimen Number:	1	2	3	4	5	6
Gender:	(F)	(F)	(F)	(F)	(M)	(F)
Skinfolds (mm):						
Chest 1	X	X	X	X	3.0	X
Abdominal 2	X	X	X	X	7.4	X
Suprailium	12.8	50.0	5.8	11.2	X	50.0
Triceps	20.2	20.8	7.4	15.2	X	14.6
Mid thigh	18.2	43.4	11.0	10.2	6.0	41.6
Σ of 3 Skinfolds:	51.2	114.2	24.2	36.6	16.4	106.2
Age (yrs.):	87	80	97	88	81	91
Body Density (g/L):	1.043	1.005	1.063	1.054	1.075	1.007
Percent Fat:	24.8	42.6	15.6	19.7	10.3	41.4

Note: X denotes variable not used in gender specific calculation.

Body Density Formulae:

Male = $1.1093800 - 0.0008267 (\Sigma 3_M) + 0.0000016 (\Sigma 3_M)^2 - 0.0002574 (\text{age})$

Female = $1.099421 - 0.0009929 (\Sigma 3_F) + 0.0000023 (\Sigma 3_F)^2 - 0.0001392 (\text{age})$

Estimation of Percent Body Fat Formula:

Siri = $[(4.95)/\text{Body Density}] - 4.5 \times 100$

MUSCLE MASS ESTIMATION

Martin (1990)

Specimen Number:	1	2	3	4	5	6
Gender:	(F)	(F)	(F)	(F)	(M)	(F)
Girths and Skinfolts (cm):						
Max forearm girth	22.5	28.2	17.7	20.2	23.3	24.4
Mid thigh girth	46.3	56.9	34.0	39.7	38.6	46.3
Max calf girth	26.9	37.4	25.5	27.7	28.6	30.8
Mid thigh skinfold	1.82	4.34	1.10	1.02	0.60	4.16
Medial calf skinfold	1.58	5.00	1.24	1.18	0.42	2.02
FG (cm):	22.5	28.2	17.7	20.2	23.3	24.4
CTG (cm):	40.58	43.27	30.54	36.50	36.72	33.23
CCG (cm):	21.94	21.69	21.60	23.99	27.28	24.45
Height (cm):	155.4	164.5	163.4	159.2	167.4	154.4
Body Mass (kg):	48.7	89.2	42.9	55.8	51.4	54.1
Muscle Mass (kg):	11.77	14.68	6.03	9.34	10.11	7.06
Muscle Mass (%):	24.2	16.5	14.1	16.7	19.7	13.1

Note: FG = forearm girth; CTG = corrected thigh girth; CCG = corrected calf girth

Estimation of Muscle Mass Formula:

$$\text{kg Muscle} = [\text{ht} * (0.0553\text{CTG}^2 + 0.0987\text{FG}^2 + 0.0331\text{CCG}^2) - 2445] * 0.001$$

$$\% \text{ Muscle} = (\text{kg muscle/body mass}) * 100$$

Matiegka (1921)

Specimen Number:	1	2	3	4	5	6
Gender:	(F)	(F)	(F)	(F)	(M)	(F)
Girths and Skinfolts (cm):						
Max upper arm girth	24.0	32.3	18.0	22.0	24.0	27.4
Max forearm girth	22.5	28.2	17.7	20.2	23.3	24.4
Mid thigh girth	46.3	56.9	34.0	39.7	38.6	46.3
Max calf girth	26.6	37.4	25.5	27.7	28.6	30.8
Triceps skinfold	2.02	2.08	0.74	1.52	0.56	1.46
Forearm 1 skinfold	0.44	2.62	0.46	0.70	0.48	1.32
Forearm 2 skinfold	0.44	2.58	0.46	0.60	0.38	1.00
Mid thigh skinfold	1.82	4.34	1.10	1.02	0.60	4.16
Mid calf skinfold	1.56	5.00	1.24	1.60	0.42	2.52
CDU (cm):	5.62	8.20	4.99	5.48	7.08	7.26
CDF (cm):	6.72	6.38	5.17	5.78	6.99	6.61
CDT (cm):	12.92	13.77	9.72	11.62	11.69	10.58
CDC (cm):	7.00	6.91	6.52	7.18	8.68	7.28
Height (cm):	155.4	164.5	163.4	159.2	167.4	154.4
Body Mass (kg):	48.7	89.2	42.9	55.8	51.4	54.1
Muscle Mass (kg):	16.43	20.76	11.57	14.61	20.16	15.79
Muscle Mass (%):	33.7	23.3	26.0	26.2	39.2	29.2

Note: CD = corrected diameter of U = upper arm; CDF = forearm; CDT = thigh; CDC = calf

Estimation of Muscle Mass Formula:

$$\text{kg muscle} = [(\text{CDU} + \text{CDF} + \text{CDT} + \text{CDC})/8]^2 * \text{ht (cm)} * 6.5 * 0.001$$

$$\% \text{ muscle} = (\text{kg muscle} / \text{body mass}) * 100$$

SKELETAL MASS ESTIMATION

Matiegka (1921)

Specimen Number:	1	2	3	4	5	6
Gender:	(F)	(F)	(F)	(F)	(M)	(F)
Breadths (cm):						
Biepicondylar humerus	6.5	5.5	6.1	6.3	6.5	6.3
Bistylodius	4.8	4.5	4.1	5.0	5.0	5.0
Biepicondylar femoral	9.2	9.4	8.6	8.5	9.6	8.8
Bimalleolar	6.2	6.6	6.6	6.5	7.1	6.4
Height (cm):	155.4	164.5	163.4	159.2	167.4	154.4
Body Mass (kg):	48.7	89.2	42.9	55.8	51.4	54.1
Skeletal Mass (kg):	8.31	8.34	7.91	8.26	9.98	8.13
Skeletal Mass (%):	17.1	9.4	18.4	14.8	19.4	15.0

Note: HB = biepicondylar humerus; WB = styloideus; FB = biepicondylar femur; AB = bimalleolar; ht = height in cm

Estimation of Skeletal Mass Formula:

$$\text{kg skeleton} = [(\text{HB} + \text{WB} + \text{FB} + \text{AB})/4]^2 * \text{ht} * 1.2\text{kg} * 0.001$$

$$\% \text{ skeleton} = (\text{kg skeleton} / \text{body mass}) * 100$$

Drinkwater (1986)

Specimen Number:	1	2	3	4	5	6
Gender:	(F)	(F)	(F)	(F)	(M)	(F)
Breadths (cm):						
Biepicondylar humerus	6.5	5.5	6.1	6.3	6.5	6.3
Bistylodius	4.8	4.5	4.1	5.0	5.0	5.0
Biepicondylar femoral	9.2	9.4	8.6	8.5	9.6	8.8
Bimalleolar	6.2	6.6	6.6	6.5	7.1	6.4
Height (cm):						
	155.4	164.5	163.4	159.2	167.4	154.4
Body Mass (kg):						
	48.7	89.2	42.9	55.8	51.4	54.1
Skeletal Mass (kg):						
	6.37	6.39	6.06	6.33	7.65	6.23
Skeletal Mass (%):						
	13.1	7.2	14.1	11.4	14.9	11.5

Note: HB = biepicondylar humerus; WB = styloideus; FB = biepicondylar femur; AB = bimalleolar; ht = height in cm

Estimation of Skeletal Mass Formula:

$$\text{kg skeleton} = [(\text{HB} + \text{WB} + \text{FB} + \text{AB})/4]^2 * \text{ht} * 0.92\text{kg} * 0.001$$

$$\% \text{ skeleton} = (\text{kg skeleton} / \text{body mass}) * 100$$

APPENDIX C

Lipid Extraction Data

The following includes a detailed report of the data collected using organic solvent lipid extraction methods.

Specimen Number: 1

Segment: Upper Arm

Tissue Mass	Dry Test	Wet Test	Difference Test	Percent Lipid
(g)	Tube Mass	Tube Mass	Tube Mass	
	(g)	(g)	(g)	
1.172	50.670	50.768	0.098	8.362
1.009	50.978	51.042	0.064	6.343
1.148	51.019	51.096	0.077	6.707
1.170	50.734	50.757	0.023	1.966
1.037	50.683	50.699	0.016	1.543
1.062	50.760	50.817	0.057	5.367

Segment Mean: 5.048

Segment: Forearm

Tissue Mass	Dry Test	Wet Test	Difference Test	Percent Lipid
(g)	Tube Mass	Tube Mass	Tube Mass	
	(g)	(g)	(g)	
1.072	50.779	50.811	0.032	2.985
1.118	50.747	50.832	0.085	7.603
1.147	50.949	50.965	0.016	1.395
1.102	50.781	50.891	0.110	9.982
1.020	50.595	50.668	0.073	7.157
1.128	51.065	51.118	0.053	4.699

Segment Mean: 5.673

Specimen: 1

Segment: Upper Leg

Tissue Mass	Dry Test Tube Mass	Wet Test Tube Mass	Difference Test Tube Mass	Percent Lipid
(g)	(g)	(g)	(g)	
1.050	50.714	50.747	0.033	3.143
1.156	50.464	50.520	0.056	4.844
1.089	50.990	51.051	0.061	5.601
1.165	50.923	50.979	0.056	4.807
1.152	50.911	50.943	0.032	2.778
1.070	50.802	50.861	0.059	5.514

Segment Mean: 4.448

Segment: Lower Leg

Tissue Mass	Dry Test Tube Mass	Wet Test Tube Mass	Difference Test Tube Mass	Percent Lipid
(g)	(g)	(g)	(g)	
1.073	50.776	50.831	0.055	5.126
1.040	51.029	51.078	0.049	4.712
1.152	50.709	50.771	0.062	5.382
1.165	50.894	50.992	0.098	8.412
1.145	50.972	51.012	0.040	3.493
1.164	50.920	50.961	0.041	3.522

Segment Mean: 5.108

Specimen Mean: 5.060

Specimen Number: 2

Segment: Upper Arm

Tissue Mass	Dry Test	Wet Test	Difference Test	Percent Lipid
(g)	Tube Mass	Tube Mass	Tube Mass	
(g)	(g)	(g)	(g)	
1.137	50.808	50.910	0.102	8.971
1.049	50.735	50.964	0.229	21.830
1.088	50.564	50.775	0.211	19.393
1.150	50.868	50.980	0.112	9.739
1.166	50.888	51.037	0.149	12.779
1.087	50.602	50.717	0.115	10.580

Segment Mean: 13.882

Segment: Forearm

Tissue Mass	Dry Test	Wet Test	Difference Test	Percent Lipid
(g)	Tube Mass	Tube Mass	Tube Mass	
(g)	(g)	(g)	(g)	
1.112	49.754	49.880	0.126	11.331
1.133	50.920	51.058	0.138	12.180
1.192	49.587	49.826	0.239	20.050
1.054	50.894	51.140	0.246	23.340
1.059	49.663	49.780	0.117	11.048
1.193	50.458	50.692	0.134	19.614

Segment Mean: 16.261

Specimen: 2

Segment: Upper Leg

Tissue Mass	Dry Test	Wet Test	Difference Test	Percent Lipid
(g)	Tube Mass	Tube Mass	Tube Mass	
	(g)	(g)	(g)	
1.191	50.152	50.258	0.105	8.816
1.097	50.837	50.896	0.059	5.378
1.048	50.462	50.530	0.068	6.489
1.191	50.860	50.988	0.128	10.747
1.103	50.499	50.700	0.201	18.223
1.065	50.844	50.892	0.048	4.507

Segment Mean: 9.027

Segment: Lower Leg

Tissue Mass	Dry Test	Wet Test	Difference Test	Percent Lipid
(g)	Tube Mass	Tube Mass	Tube Mass	
	(g)	(g)	(g)	
1.616	50.652	50.808	0.156	13.437
1.058	50.910	51.013	0.103	9.735
1.167	51.038	51.157	0.119	10.197
1.143	50.716	50.976	0.260	22.747
1.186	50.809	50.906	0.097	8.179
1.072	50.988	51.323	0.335	31.250

Segment Mean: 15.924

Specimen Mean: 13.773

Specimen Number: 3

Segment: Upper Arm

Tissue Mass	Dry Test	Wet Test	Difference Test	Percent Lipid
(g)	Tube Mass	Tube Mass	Tube Mass	
(g)	(g)	(g)	(g)	
1.163	50.552	50.642	0.090	7.739
1.126	50.860	50.894	0.034	3.020
1.044	50.773	50.858	0.085	8.142
1.073	50.793	50.888	0.095	8.854
1.141	50.586	50.705	0.119	10.429
1.199	51.114	51.209	0.095	7.923

Segment Mean: 7.684

Segment: Forearm

Tissue Mass	Dry Test	Wet Test	Difference Test	Percent Lipid
(g)	Tube Mass	Tube Mass	Tube Mass	
(g)	(g)	(g)	(g)	
1.086	49.976	50.112	0.136	12.523
1.043	50.589	50.720	0.131	12.560
1.040	50.849	50.954	0.105	10.096
1.002	50.755	50.885	0.130	12.974
1.128	50.713	50.882	0.169	14.982
1.024	50.871	50.956	0.085	8.301

Segment Mean: 11.906

Specimen: 3

Segment: Upper Leg

Tissue Mass	Dry Test	Wet Test	Difference Test	Percent Lipid
(g)	Tube Mass	Tube Mass	Tube Mass	
1.072	50.786	50.998	0.212	19.776
1.910	50.372	50.608	0.236	19.832
1.172	50.769	50.992	0.223	19.027
1.003	50.822	50.944	0.122	12.164
1.088	50.847	51.010	0.163	14.982
1.097	50.711	50.946	0.235	21.422

Segment Mean: 17.867

Segment: Lower Leg

Tissue Mass	Dry Test	Wet Test	Difference Test	Percent Lipid
(g)	Tube Mass	Tube Mass	Tube Mass	
1.132	50.854	51.074	0.220	19.435
1.184	50.823	50.981	0.158	13.345
1.123	50.763	50.934	0.171	15.227
1.171	51.002	51.091	0.089	7.600
1.180	50.668	50.875	0.207	17.542
1.178	50.979	51.124	0.145	12.309

Segment Mean: 14.243

Specimen Mean: 12.925

Specimen Number: 4

Segment: Upper Arm

Tissue Mass	Dry Test	Wet Test	Difference Test	Percent Lipid
(g)	Tube Mass	Tube Mass	Tube Mass	
	(g)	(g)	(g)	
1.026	50.514	50.596	0.082	7.992
1.051	50.485	50.609	0.124	11.798
1.025	50.921	51.008	0.087	8.488
1.162	50.822	50.928	0.106	9.122
1.107	50.831	50.991	0.160	14.453
1.248	50.735	50.805	0.070	5.609

Segment Mean: 9.577

Segment: Forearm

Tissue Mass	Dry Test	Wet Test	Difference Test	Percent Lipid
(g)	Tube Mass	Tube Mass	Tube Mass	
	(g)	(g)	(g)	
1.240	50.756	50.827	0.071	5.726
1.091	50.932	50.994	0.062	5.683
1.062	50.634	50.674	0.040	3.766
1.022	50.887	50.964	0.077	7.534
1.049	50.893	50.950	0.057	5.434
1.041	50.827	50.880	0.053	5.091

Segment Mean: 5.539

Specimen: 4

Segment: Upper Leg

Tissue Mass	Dry Test Tube Mass	Wet Test Tube Mass	Difference Test Tube Mass	Percent Lipid
(g)	(g)	(g)	(g)	
1.028	50.892	50.951	0.059	5.739
1.022	50.659	50.699	0.040	3.914
1.183	50.727	50.792	0.065	5.495
1.028	50.833	50.863	0.030	2.918
1.038	50.912	51.011	0.099	9.538
1.050	50.537	50.605	0.068	6.476
Segment Mean:				5.680

Segment: Lower Leg

Tissue Mass	Dry Test Tube Mass	Wet Test Tube Mass	Difference Test Tube Mass	Percent Lipid
(g)	(g)	(g)	(g)	
1.181	50.878	50.957	0.079	6.689
1.116	50.579	50.626	0.047	4.211
1.069	49.920	49.979	0.059	5.519
1.149	51.013	51.066	0.053	4.613
1.080	50.621	50.679	0.058	5.370
1.025	50.145	50.164	0.019	1.854
Segment Mean:				4.709

Specimen Mean: 6.376

Specimen Number: 5

Segment: Upper Arm

Tissue Mass	Dry Test	Wet Test	Difference Test	Percent Lipid
(g)	Tube Mass	Tube Mass	Tube Mass	
(g)	(g)	(g)	(g)	
1.177	50.838	50.976	0.138	11.725
1.178	50.493	50.609	0.116	9.847
1.033	50.560	50.612	0.052	5.034
1.075	50.836	50.906	0.070	6.512
1.093	50.884	50.912	0.028	2.562
1.067	50.597	50.643	0.046	4.311

Segment Mean: 6.665

Segment: Forearm

Tissue Mass	Dry Test	Wet Test	Difference Test	Percent Lipid
(g)	Tube Mass	Tube Mass	Tube Mass	
(g)	(g)	(g)	(g)	
1.016	49.751	49.852	0.101	9.941
1.061	50.911	51.067	0.156	14.703
1.080	49.582	49.634	0.052	4.815
1.198	50.894	50.964	0.070	5.843
1.069	49.664	49.734	0.070	6.548
1.117	50.455	50.526	0.071	6.356

Segment Mean: 8.034

Specimen: 5

Segment: Upper Leg

Tissue Mass	Dry Test	Wet Test	Difference Test	Percent Lipid
(g)	Tube Mass	Tube Mass	Tube Mass	
1.172	50.148	50.220	0.072	6.143
1.047	50.749	50.809	0.060	5.731
1.105	50.460	50.540	0.080	7.240
1.161	50.695	50.760	0.065	5.598
1.000	50.479	50.554	0.075	7.500
1.048	50.769	50.834	0.065	16.202

Segment Mean: 6.402

Segment: Lower Leg

Tissue Mass	Dry Test	Wet Test	Difference Test	Percent Lipid
(g)	Tube Mass	Tube Mass	Tube Mass	
1.100	50.510	50.628	0.118	10.727
1.038	50.757	50.846	0.089	7.821
1.126	49.703	49.781	0.078	6.927
1.076	50.675	50.774	0.099	9.201
1.180	50.756	50.853	0.097	8.220
1.123	50.895	50.997	0.012	9.083

Segment Mean: 8.663

Specimen Mean: 7.441

Specimen Number: 6

Segment: Upper Arm

Tissue Mass	Dry Test	Wet Test	Difference Test	Percent Lipid
(g)	Tube Mass	Tube Mass	Tube Mass	
(g)	(g)	(g)	(g)	
1.077	50.572	50.695	0.123	11.421
1.235	50.869	51.020	0.151	12.227
1.086	50.919	51.086	0.167	15.378
1.013	50.631	50.775	0.144	14.215
1.133	50.587	X	X	X
1.215	50.728	X	X	X

Segment Mean: 13.310

Segment: Forearm

Tissue Mass	Dry Test	Wet Test	Difference Test	Percent Lipid
(g)	Tube Mass	Tube Mass	Tube Mass	
(g)	(g)	(g)	(g)	
1.267	50.748	50.896	0.148	11.681
1.156	50.601	50.710	0.109	9.429
1.206	50.852	50.973	0.121	10.033
1.327	50.761	50.875	0.114	8.591
1.253	50.716	50.847	0.131	10.455
1.133	50.873	51.018	0.145	12.798

Segment Mean: 10.498

Note: X = data was not available as test-tube shattered.

Specimen: 6

Segment: Upper Leg

Tissue Mass	Dry Test	Wet Test	Difference Test	Percent Lipid
(g)	Tube Mass	Tube Mass	Tube Mass	
(g)	(g)	(g)	(g)	
1.083	50.565	50.681	0.116	10.711
1.219	50.830	51.111	0.288	23.052
1.101	51.074	51.139	0.065	5.904
1.169	50.767	50.898	0.131	11.206
1.065	50.794	50.984	0.190	17.840
1.067	51.005	51.199	0.194	18.182

Segment Mean: 14.482

Segment: Lower Leg

Tissue Mass	Dry Test	Wet Test	Difference Test	Percent Lipid
(g)	Tube Mass	Tube Mass	Tube Mass	
(g)	(g)	(g)	(g)	
1.165	50.151	50.357	0.206	17.682
1.188	50.763	50.976	0.213	17.929
1.149	50.586	50.745	0.159	13.838
1.154	50.719	50.826	0.107	9.272
1.083	50.616	50.714	0.098	9.049
1.040	50.842	50.973	0.131	12.596

Segment Mean: 13.395

Specimen Mean: 12.886

APPENDIX D

Magnetic Resonance Data - CSI

The following includes a detailed report of the data collected using magnetic resonance imaging methods (CSI) and the mathematical analysis used to arrive at the values presented.

Percent fat values were calculated by expressing the fat signal as a percentage of the total signal number. Total signal was determined by multiplication of total signal mean square value by the number of signal points identified in the analysis. Fat signal was calculated in a similar manner by multiplying the fat signal mean square value by the number of points.

The data for all specimens is presented with the upper arm segment first and finishing with the lower leg segment.

Specimen Number:	1	2	3	4	5	6
Segment: Upper Arm						
Coordinates:						
X-axis:	92	98	92	92	100	104
Y-axis:	83	94	88	84	90	82
Width:	70	45	70	70	60	60
Height:	70	50	70	70	60	32
Number of points:	4900	2250	4900	4900	3600	1920
Total signal mean square:	1.030	3.343	1.577	0.595	1.306	0.509
Total signal:	5047.2	7522.2	7729.6	2917.9	4700.0	977.7
2 Fat signal mean square:	0.134	0.857	0.282	0.064	0.108	0.095
Fat signal mean square:	0.067	0.429	0.141	0.032	0.054	0.047
Fat signal:	328.1	964.6	690.3	156.0	194.3	90.8
Percent Fat:	6.501	12.823	8.930	5.347	4.134	9.290

Specimen Number:	1	2	3	4	5	6
Segment: Forearm						
Coordinates:						
X-axis:	92	92	92	102	102	105
Y-axis:	83	84	88	94	109	94
Width:	70	70	70	50	50	50
Height:	70	70	70	45	32	32
Number of points:	4900	4900	4900	2250	1600	1600
Total signal mean square:	1.219	1.747	2.009	2.234	2.863	7.015
Total signal:	5974.2	8560.1	9846.5	5027.0	4580.5	11223.9
2 Fat signal mean square:	0.101	0.558	0.521	0.172	0.860	1.904
Fat signal mean square:	0.050	0.279	0.261	0.086	0.430	0.952
Fat signal:	246.4	1365.9	1276.7	193.3	687.8	1522.9
Percent Fat:	4.125	15.957	12.966	3.844	15.016	13.568

Specimen Number:	1	2	3	4	5	6
Segment: Upper Leg						
Coordinates:						
X-axis:	91	87	77	76	78	80
Y-axis:	66	50	68	59	62	57
Width:	70	105	40	90	90	100
Height:	70	100	60	90	90	100
Number of points:	4900	10500	2400	8100	8100	10000
Total signal mean square:	1.271	0.202	0.163	0.352	0.290	0.305
Total signal:	6230.0	2125.4	390.9	2854.5	2347.0	3052.4
2 Fat signal mean square:	0.063	0.054	0.063	0.126	0.042	0.092
Fat signal mean square:	0.032	0.027	0.031	0.063	0.021	0.046
Fat signal:	155.5	285.7	75.4	510.5	168.7	459.5
Percent Fat:	2.496	13.441	19.291	17.885	7.189	15.054

Specimen Number:	1	2	3	4	5	6
Segment: Lower Leg						
Coordinates:						
X-axis:	92	90	87	94	91	103
Y-axis:	83	96	86	107	87	86
Width:	70	45	70	60	65	60
Height:	70	50	70	32	65	60
Number of points:	4900	2250	4900	1920	4225	3600
Total signal mean square:	2.047	1.945	1.664	0.261	1.195	2.491
Total signal:	10029.6	4375.9	8154.7	501.0	5046.9	8968.7
2 Fat signal mean square:	0.178	0.625	0.627	0.034	0.175	0.150
Fat signal mean square:	0.089	0.312	0.314	0.017	0.088	0.075
Fat signal:	435.6	702.9	1537.0	32.6	370.7	270.4
	4.344	16.062	18.848	6.506	7.345	3.015